$C_{21}H_{21}Na_2O_3$: 367.1286). Anal. Calcd for $C_{21}H_{21}NaO_3 \cdot 0.5H_2O$: C, 71.22; H, 6.36. Found: C, 71.37, H, 6.27.

5.2.3.4. Sodium 2-{4′-methyl-5-[(2-oxocyclopentyl)methyl]biphenyl-2-yl}propanoate (25). Yield: 77%, three steps. IR (KBr) ν: 1420, 1712 (CO_2^-), 1733 (C=O), cm $^{-1}$. ^{1}H NMR (CD_3OD) δ: 1.21 (3H, dd, J = 7.3, 1.5 Hz, α-CH_3), 1.54–2.44 (7H, m, H1′, H3′, H4′, H5′), 2.36 (3H, s, Ar-CH_3), 2.51 (1H, dd, J = 13.4, 9.3 Hz, CH_2), 3.04 (1H, dd, J = 13.7, 9.3 Hz, CH_2), 3.72 (1H, q, J = 7.1 Hz, CH), 6.92 (1H, t, J = 1.8 Hz, Ar-H3), 7.08 (1H, dt, J = 8.1, 1.8 Hz, Ar-H5), 7.18 (2H, d, J = 7.7 Hz, Ar-H3′), 7.26 (2H, d, J = 7.7 Hz, Ar-H2′), 7.44 (1H, d, J = 8.1 Hz, Ar-H6). ^{13}C NMR (CD_3OD) δ: 21.19 (α-CH_3), 21.47 (C5′), 21.44 (C4′), 30.08 (Ar-CH_3), 36.07 (CH_2), 39.08 (C3′), 45.70 (CH), 52.12 (C1′), 128.61 (Ar-C1), 128.80 (Ar-C5), 129.58 (Ar-C2′), 130.53 (Ar-C3′), 131.31 (Ar-C6), 137.33 (Ar-C3), 138.29 (Ar-C4′), 140.52 (Ar-C2), 141.64 (Ar-C1′), 143.09 (Ar-C4), 183.58 (CO_2Na), 223.09 (C=O). HR-FAB-MS (m/z): 381.1439 (M^++Na, calcd for $C_{22}H_{23}Na_2O_3$: 381.1443). Anal. Calcd for $C_{22}H_{23}NaO_3 \cdot 0.5H_2O$: C, 72.03; H, 6.66. Found: C, 71.92, H, 6.58.

5.2.3.5. Sodium 2-{4′-methoxy-5-[(2-oxocyclopentyl)methyl]biphenyl-2-yl}propanoate (26). Yield: 70%, three steps. IR (KBr) ν: 1416, 1711 (CO_2^-), 1732 (C=O), cm^{-1}. ^{1}H NMR (CD_3OD) δ: 1.22 (3H, dd, J = 7.0, 1.5 Hz, α-CH_3), 1.53–2.40 (7H, m, H1′, H3′, H4′, H5′), 2.51 (1H, dd, J = 13.6, 9.5 Hz, CH_2), 3.04 (1H, dd, J = 13.4, 3.8 Hz, CH_2), 3.73 (1H, q, J = 7.0 Hz, CH), 3.81 (3H, s, Ar-OCH_3), 6.92–6.95 (3H, m, Ar-H3, Ar-H3′), 7.07 (1H, d, J = 8.1 Hz, Ar-H5), 7.31 (2H, d, J = 8.4 Hz, Ar-H2′), 7.43 (1H, d, J = 8.1 Hz, Ar-H6). ^{13}C NMR (CD_3OD) δ: 21.23 (α-CH_3), 21.45 (C5′), 30.08 (C4′), 36.08 (CH_2), 39.09 (C3′), 45.70 (CH), 52.03 (C1′), 55.72 (Ar-OCH_3), 114.43 (Ar-C2′), 128.60 (Ar-C1), 128.72 (Ar-C5), 131.44 (Ar-C6), 131.70 (Ar-C3′), 135.81 (Ar-C3), 138.29 (Ar-C4′), 141.73 (Ar-C2), 142.78 (Ar-C1′), 160.07 (Ar-C4), 183.60 (CO_2Na), 223.10 (C=O). HR-FAB-MS (m/z): 397.1399 (M^++Na, calcd for $C_{22}H_{23}Na_2O_4$: 397.1392). Anal. Calcd for $C_{22}H_{23}NaO_4 \cdot H_2O$: C, 67.22; H, 6.38. Found: C, 67.33, H, 6.42.

5.2.3.6. Sodium 2-(4′-(methylthio)-5-((2-oxocyclopentyl)methyl)biphenyl-2-yl)propanoate (27). Yield: 60%, three steps. IR (KBr) ν: 1417, 1712 (CO_2^-), 1730 (C=O), cm $^{-1}$. ^{1}H NMR (CD_3OD) δ: 1.23 (3H, dd, J = 7.1, 1.3 Hz, α-CH_3), 1.55–2.45 (7H, m, H1′, H3′, H4′, H5′), 2.49 (3H, s, Ar-SCH_3), 2.52 (1H, dd, J = 13.9, 9.2 Hz, CH_2), 3.05 (1H, dd, J = 13.6, 4.0 Hz, CH_2), 3.70 (1H, q, J = 7.2 Hz, CH), 6.94 (1H, t, J = 1.8 Hz, Ar-H3), 7.10 (1H, dt, J = 8.1, 2.2 Hz, Ar-H5), 7.31 (4H, dd, J = 14.5, 8.6 Hz, Ar-H2′, Ar-H3′), 7.45 (1H, d, J = 8.1 Hz, Ar-H6). ^{13}C NMR (CD_3OD) δ: 15.91 (Ar-SCH_3), 21.21 (α-CH_3), 21.45 (C5′), 30.09 (C4′), 36.06 (CH_2), 39.06 (C3′), 45.73 (CH), 52.12 (C1′), 127.36 (Ar-C3′), 128.70 (Ar-C1), 128.98 (Ar-C5), 129.05 (Ar-C6), 131.17 (Ar-C2′), 138.33 (Ar-C3), 138.44 (Ar-C2), 140.32 (Ar-C1′), 141.61 (Ar-C4), 142.49 (Ar-C4′), 183.42 (CO_2Na), 223.01 (C=O). HR-FAB-MS (m/z): 413.1165 (M^++Na, calcd for $C_{22}H_{23}Na_2SO_3$: 413.1163). Anal. Calcd for $C_{22}H_{23}NaSO_3 \cdot H_2O$: C, 64.54; H, 6.10. Found: C, 64.69, H, 6.17.

5.2.3.7. Sodium 2-{4′-fluoro-5-[(2-oxocyclopentyl)methyl]biphenyl-2-yl}propanoate (28). Yield: 64%, three steps. IR (KBr) ν: 1204 (Ar-F), 1414, 1710 (CO_2^-), 1730 (C=O), cm^{-1}. ^{1}H NMR (CD_3OD) δ: 1.22 (3H, dd, J = 7.3, 1.1 Hz, α-CH_3), 1.55–2.41 (7H, m, H1′, H3′, H4′, H5′), 2.52 (1H, dd, J = 13.6, 9.2 Hz, CH_2), 3.05 (1H, dd, J = 13.6, 4.0 Hz, CH_2), 3.64 (1H, q, J = 7.2 Hz, CH), 6.93 (1H, t, J = 1.8 Hz, Ar-H3), 7.13–7.07 (3H, m, Ar-H5, Ar-H3′), 7.38–7.46 (3H, m, Ar-H6, Ar-H2′). ^{13}C NMR (CD_3OD) δ: 21.08 (α-CH_3), 21.45 (C5′), 30.09 (C4′), 36.04 (CH_2), 39.06 (C3′), 45.73 (CH), 52.09 (C1′), 115.60 (d, J_{C-F} = 21.1 Hz, Ar-C3′), 128.68 (Ar-C1), 129.19 (Ar-C5), 131.32 (Ar-C6), 132.46 (d, J_{C-F} = 8.1 Hz, Ar-C2′), 138.50 (Ar-C3), 139.57 (d, J_{C-F} = 3.7 Hz, Ar-C1′), 141.64 (Ar-C2), 142.02 (Ar-C4), 142.49 (d, J_{C-F} = 1.9 Hz, Ar-C4′), 183.28 (CO_2Na), 222.98 (C=O). HR-FAB-MS (m/z): 385.1188 (M^++Na, calcd for $C_{21}H_{20}FNa_2O_3$: 385.1192). Anal. Calcd for $C_{21}H_{20}FNaO_3 \cdot H_2O$: C, 66.31; H, 5.83. Found: C, 66.44, H, 5.76.

5.2.3.8. Sodium 2-{5-[(2-oxocyclopentyl)methyl]-4′-(trifluoromethoxy)biphenyl-2-yl}propanoate (29). Yield: 56%, three steps. IR (KBr) ν: 1421, 1709 (CO_2^-), 1731 (C=O), cm $^{-1}$. ^{1}H NMR (CD_3OD) δ: 1.25 (3H, dd, J = 7.0, 1.1 Hz, α-CH_3), 1.51–2.45 (7H, m, H1′, H3′, H4′, H5′), 2.53 (1H, dd, J = 13.6, 9.5 Hz, CH_2), 3.05 (1H, dd, J = 13.6, 4.0 Hz, CH_2), 3.62 (1H, q, J = 7.2 Hz, CH), 6.95 (1H, t, J = 2.2 Hz, Ar-H3), 7.13 (1H, dt, J = 8.1, 2.2 Hz, Ar-H3′), 7.28 (2H, dd, J = 8.8, 0.7 Hz, Ar-H5,), 7.46–7.51 (3H, m, Ar-H6, Ar-H2′). ^{13}C NMR (CD_3OD) δ: 21.12 (α-CH_3), 21.44 (C5′), 30.08 (C4′), 35.99 (CH_2), 39.04 (C3′), 47.75 (CH), 52.04 (C1′), 121.51 (Ar-C3′), 128.77 (Ar-C1), 129.46 (Ar-C5), 131.17 (Ar-OCF_3), 131.23 (Ar-C6), 132.37 (Ar-C2′), 138.62 (Ar-C1′), 141.52 (Ar-C3), 141.57 (Ar-C2), 142.58 (Ar-C4),, 149.45 (Ar-C4′), 183.28 (CO_2Na), 222.98 (C=O). HR-FAB-MS (m/z): 451.1107 (M^++Na, calcd for $C_{22}H_{20}F_3Na_2O_4$: 451.1109). Anal. Calcd for $C_{22}H_{20}F_3NaO_4 \cdot 0.5H_2O$: C, 60.41; H, 4.84. Found: C, 60.34, H, 4.98.

5.2.3.9. Sodium 2′-(1-carboxylatoethyl)-5′-[(2-oxocyclopentyl)-methyl]biphenyl-4-carboxylate (30). Yield: 74%, three steps. IR (KBr) ν: 1420, 1689, 1712 (CO_2^-), 1727 (C=O), cm $^{-1}$. ^{1}H NMR (CD_3OD) δ: 1.22 (3H, dd, J = 7.1, 1.6 Hz, α-CH_3), 1.33–2.42 (7H, m, H1′, H3′, H4′, H5′), 2.53 (1H, dd, J = 13.6, 9.2 Hz, CH_2), 3.06 (1H, dd, J = 13.6, 4.0 Hz, CH_2), 3.73 (1H, q, J = 7.1 Hz, CH), 6.96 (1H, st, J = 1.6 Hz, Ar-H3), 7.11 (1H, dt, J = 8.1, 1.8 Hz, Ar-H5), 7.40 (2H, d, J = 8.4 Hz, Ar-H2′), 7.44 (1H, d, J = 8.1 Hz, Ar-H6), 7.99 (2H, d, J = 8.4 Hz, Ar-H3′). ^{13}C NMR (CD_3OD) δ: 20.00 (α-CH_3), 21.45 (C5′), 30.11 (C4′), 36.06 (CH_2), 39.05 (C3′), 45.55 (CH), 52.11 (C1′), 128.64 (Ar-C1), 129.18 (Ar-C5′), 130.01 (Ar-C2′), 130.10 (Ar-C3′), 131.23 (Ar-C6), 137.37 (Ar-C3), 138.52 (Ar-C2), 141.47 (Ar-C4′), 142.81 (Ar-C4), 145.50 (Ar-C1′), 175.36 (Ar-CO_2Na), 183.17 (CO_2Na), 223.02 (C=O). HR-FAB-MS (m/z): 433.1001 (M^++Na, calcd for $C_{22}H_{20}Na_3O_5$: 433.1004). Anal. Calcd for $C_{22}H_{20}Na_2O_5 \cdot H_2O$: C, 61.68; H, 5.18. Found: C, 61.54, H, 5.06.

5.2.3.10. Sodium 2-{4′-hydroxy-5-[(2-oxocyclopentyl)methyl]-biphenyl-2-yl}propanoate (31). Yield: 50%, three steps. IR (KBr) ν: 1318 (Ar-OH), 1421, 1710 (CO_2^-), 1731 (C=O), cm^{-1}. ^{1}H NMR (CD_3OD) δ: 1.22 (3H, dd, J = 7.3, 1.5 Hz, α-CH_3), 1.52–2.42 (7H, m, H1′, H3′, H4′, H5′), 2.50 (1H, d, J = 13.9 Hz, CH_2), 3.02 (1H, d, J = 13.6 Hz, CH_2), 3.75 (1H, q, J = 7.2 Hz, CH), 6.80 (2H, d, J = 8.4 Hz, Ar-H3′), 6.92 (1H, s, Ar-H3), 7.05 (1H, d, J = 8.1 Hz, Ar-H5), 7.21 (2H, d, J = 8.4 Hz, Ar-H2′), 7.42 (1H, d, J = 8.1 Hz, Ar-H6). ^{13}C NMR (CD_3OD) δ: 21.32 (α-CH_3), 30.10 (C5′), 36.10 (C4′), 39.09 (CH_2), 45.72 (C3′), 52.20 (CH), 58.31 (C1′), 116.15 (Ar-C3′), 128.40 (Ar-C1), 128.54 (Ar-C5), 131.51 (Ar-C6), 131.66 (Ar-C2′), 134.03 (Ar-C1′), 138.19 (Ar-C3), 141.76 (Ar-C2), 143.24 (Ar-C4), 158.47 (Ar-C4′), 183.81 (CO_2Na), 219.16 (C=O). HR-FAB-MS (m/z): 361.1414 (M^++H, calcd for $C_{21}H_{22}NaO_4$: 361.1416). Anal. Calcd for $C_{21}H_{21}NaO_4 \cdot H_2O$: C, 68.28; H, 6.00. Found: C, 68.30, H, 6.09.

5.2.4. Synthesis of the alcohol derivative of 31 (32, 33)

A methyl ester intermediate derived from **31** was reduced by $NaBH_4$ (see below) and alkaline hydrolyzed.

5.2.4.1. Reduction of methyl ester intermediate derived from 31 with $NaBH_4$. To a stirred solution of methyl ester intermediate derived from **31** (1 equiv, ca. 1.8 mmol) in EtOH, $NaBH_4$ (1.3 equiv, ca. 2.4 mmol) was added, stirred for 1 h at room temperature, quenched by the addition of a few ice chips, and the resulting solution was extracted with CH_2Cl_2. The extracts were dried over anhydrous Na_2SO_4 and filtrated. The filtrate was evaporated to

dryness, and the mixture was separated into *cis*-alcohol and *trans*-alcohol as two kinds of colorless oil by silica gel chromatography (*n*-hexane/AcOEt, 7:2) (93–95%).

5.2.4.2. (±)-2-{4′-Hydroxy-5-[(trans-2-hydroxycyclopentyl)methyl]biphenyl-2-yl}propanoic acid (32). Yield: 82%, three steps. IR (KBr) *ν*: 1321 (Ar-OH), 1421, 1714 (CO_2^-), 1733 (C=O), 3466 (OH), cm^{-1}. ^{1}H NMR (CD_3OD) *δ*: 1.27 (3H, d, *J* = 7.1 Hz, α-CH_3), 1.20–1.94 (6H, m, H3′, H4′, H5′), 1.95–2.06 (1H, m, H1′), 2.38 (1H, dd, *J* = 13.6, 9.2 Hz, CH_2), 2.85 (1H, dd, *J* = 13.6, 5.7 Hz, CH_2), 3.78–3.88 (2H, m, CH, H2′), 6.83 (2H, d, *J* = 8.4 Hz, Ar-H3′), 7.00 (1H, s, Ar-H3), 7.11–7.16 (3H, m, Ar-H5, Ar-H2′), 7.27 (1H, d, *J* = 8.1 Hz, Ar-H6), 10.57 (1H, br s, CO_2H). ^{13}C NMR (CD_3OD) *δ*: 19.72 (α-CH_3), 22.37 (C4′), 30.30 (C5′), 34.64 (CH_2), 40.11 (C3′), 42.04 (CH), 50.67 (C1′), 78.83 (C2′), 115.94 (Ar-C3′), 127.66 (Ar-C1), 128.98 (Ar-C5), 131.55 (Ar-C6), 131.88 (Ar-C3), 133.97 (Ar-C1′), 137.99 (Ar-C2′), 140.95 (Ar-C2), 143.03 (Ar-C4), 157.73 (Ar-C4′), 178.94 (CO_2H). HR-FAB-MS (*m/z*): 340.1677 (M^+, calcd for $C_{21}H_{24}O_4$: 340.1675). Anal. Calcd for $C_{21}H_{24}O_4 \cdot 0.25H_2O$: C, 73.13; H, 7.16. Found: C, 72.91, H, 7.30.

5.2.4.3. (±)-2-{4′-Hydroxy-5-[(*cis*-2-hydroxycyclopentyl)methyl]biphenyl-2-yl}propanoic acid (33). Yield: 80%, three steps. IR (KBr) *ν*: 1318 (Ar-OH), 1420, 1714 (CO_2^-), 1731 (C=O), 3466 (OH), cm^{-1}. ^{1}H NMR (CD_3OD) *δ*: 1.27 (3H, d, *J* = 7.0 Hz, α-CH_3), 1.44–1.87 (6H, m, H3′, H4′, H5′), 1.90–2.02 (1H, m, H1′), 2.56 (1H, dd, *J* = 13.4, 8.2 Hz, CH_2), 2.87 (1H, dd, *J* = 6.8, 3.4 Hz, CH_2), 3.85 (1H, q, *J* = 7.1 Hz, CH), 4.04 (1H, br s, H2′), 6.80 (2H, d, *J* = 8.4 Hz, Ar-H3′), 7.04 (1H, s, Ar-H3), 7.15 (3H, d, *J* = 8.4 Hz, Ar-H5, Ar-H2′), 7.26 (1H, d, *J* = 8.1 Hz, Ar-H6), 10.56 (1H, br s, CO_2H). ^{13}C NMR (CD_3OD) *δ*: 19.37 (α-CH_3), 22.56 (C4′), 29.62 (C5′), 35.41 (CH_2), 36.07 (C3′), 42.03 (CH), 50.67 (C1′), 75.18 (C2′), 115.92 (Ar-C3′), 127.60 (Ar-C1), 128.89 (Ar-C5), 131.56 (Ar-C6), 131.79 (Ar-C3), 134.07 (Ar-C1′), 137.77 (Ar-C2′), 141.84 (Ar-C2), 142.98 (Ar-C4), 157.69 (Ar-C4′), 178.99 (CO_2H). HR-FAB-MS (*m/z*): 340.1678 (M^+, calcd for $C_{21}H_{24}O_4$: 340.1675). Anal. Calcd for $C_{21}H_{24}O_4 \cdot 0.5H_2O$: C, 72.18; H, 7.21. Found: C, 72.35, H, 7.29.

5.3. Membrane permeability assay

Permeabilization of calcein-loaded liposomes was assayed as described previously,[14] with some modifications. Liposomes were prepared using the reversed-phase evaporation method. Egg phosphatidylcholine (PC) (10 μmol, 7.7 mg) was dissolved in chloroform/methanol (1:2, v/v), dried, dissolved in 1.5 mL of diethyl ether, and added to 1 mL of 100 mM calcein/NaOH (pH 7.4). The mixture was then sonicated to obtain a homogenous emulsion. The diethyl ether solvent was removed and the resulting suspension of liposomes was centrifuged and washed twice with fresh buffer A (10 mM phosphate buffer (Na_2HPO_4–NaH_2PO_4) (pH 6.8) containing 150 mM NaCl) to remove untrapped calcein. The final liposome precipitate was re-suspended in 5 mL buffer A. A 30 μL aliquot of this suspension was diluted with buffer A to 20 mL, and 12 or 400 μL of this diluted suspension was then incubated at 30 °C for 10 min in the presence of the compound under investigation. Control experiments were performed after addition of the same volume of water. The release of calcein from liposomes was determined by measuring the fluorescence intensity at 520 nm (excitation at 490 nm).

5.4. Human whole blood COX assay

This assay was performed as decribed[43] with some modifications. Fresh blood was collected in tubes (Protein Lobinding tube, Eppendorf Co., Ltd, Tokyo, Japan) by venipuncture from healthy volunteers who had no apparent inflammatory conditions and had not taken any NSAIDs for least 7 days prior to blood collection.

5.4.1. COX-1 assay

Aliquots of blood (500 μL) were incubated with 2 μL of test compound for 24 h at 37 °C, then centrifuged to obtain plasma. Aliquots (100 μL) of plasma were mixed with 400 μL methanol and centrifuged. The amount of TXB_2 in the supernatant was determined using an EIA kit (Cayman, Ann Arbor, MI) according to the manufacturer's protocol.

5.4.2. COX-2 assay

Blood samples (500 μL) were incubated with 100 μg/mL lipopolysaccharide (Sigma–Aldrich Japan Inc., Tokyo, Japan) for 24 h at 37 °C after addition of 2 μL of test compound, then centrifuged to obtain plasma. Aliquots (100 μL) of plasma were mixed with 400 μL methanol and centrifuged. The amount of PGE_2 in the supernatant was determined using an EIA kit (Cayman, Ann Arbor, MI) according to the manufacturer's protocol.

5.5. Gastric damage assay and determination of gastric level of PGE_2

Wistar rats (6 weeks old, 180–200 g, male) were obtained from Kyudo Co., Ltd (Kumamoto, Japan). The experiments and procedures described here were carried out in accordance with the Guide for the Care and Use of Laboratory Animals as adopted and promulgated by the National Institutes of Health (Bethesda, MD), and were approved by the Animal Care Committee of Kumamoto University.

The gastric ulcerogenic response was examined as described previously,[20] with some modifications. Rats fasted for 18 h were orally administered NSAIDs. Eight hours later, the animals were sacrificed, after which their stomachs were removed and the areas of gastric mucosal lesions were measured by an observer unaware of the treatment they had received. Calculation of the scores involved measuring the area of all the lesions in square millimeters and summing the values to give an overall gastric lesion index. The gastric PGE_2 level was determined by EIA according to the manufacturer's instructions.

5.6. Carrageenan-induced rat paw edema

This assay was carried out as described previously.[44] Rats were orally administered NSAIDs and 1 h later received a 100 μL intradermal injection of carrageenan (1%) into the left hindpaw. Paw volume was measured using a plethsysmometer, which measures water displacement when the paw is submerged in a water cell. The percentage difference in volume between both paws was shown as edema (%). The PGE_2 level in the paw was determined by EIA according to the manufacturer's instructions.

5.7. Statistical analysis

All values are expressed as the mean ± SEM. The Tukey test or the Student's *t*-test for unpaired results was used to evaluate differences between more than three groups or between two groups, respectively. Differences were considered to be significant for values of $P < 0.05$.

Acknowledgments

This work was supported by Grants-in-Aid of Scientific Research from the Ministry of Health, Labour, and Welfare of Japan, Grants-in-Aid for Scientific Research from the Ministry of

Education, Culture, Sports, Science and Technology of Japan, and Grants-in-Aid of the Japan Science and Technology Agency.

Supplementary data

Supplementary data (NMR spectra of final compounds) associated with this article can be found, in the online version, at doi:10.1016/j.bmc.2011.04.050.

References and notes

1. Smalley, W. E.; Ray, W. A.; Daugherty, J. R.; Griffin, M. R. *Am. J. Epidemiol.* **1995**, *141*, 539.
2. Singh, G. *Am. J. Med.* **1998**, *105*, 31S.
3. Kujubu, D. A.; Fletcher, B. S.; Varnum, B. C.; Lim, R. W.; Herschman, H. R. *J. Biol. Chem.* **1991**, *266*, 12866.
4. Xie, W. L.; Chipman, J. G.; Robertson, D. L.; Erikson, R. L.; Simmons, D. L. *Proc. Natl. Acad. Sci. U.S.A.* **1991**, *88*, 2692.
5. Silverstein, F. E.; Faich, G.; Goldstein, J. L.; Simon, L. S.; Pincus, T.; Whelton, A.; Makuch, R.; Eisen, G.; Agrawal, N. M.; Stenson, W. F.; Burr, A. M.; Zhao, W. W.; Kent, J. D.; Lefkowith, J. B.; Verburg, K. M.; Geis, G. S. *JAMA* **2000**, *284*, 1247.
6. Bombardier, C.; Laine, L.; Reicin, A.; Shapiro, D.; Burgos, V. R.; Davis, B.; Day, R.; Ferraz, M. B.; Hawkey, C. J.; Hochberg, M. C.; Kvien, T. K.; Schnitzer, T. J. N. *Engl. J. Med.* **2000**, *343*, 1520.
7. FitzGerald, G. A.; Patrono, C. N. *Engl. J. Med.* **2001**, *345*, 433.
8. Mukherjee, D.; Nissen, S. E.; Topol, E. J. *JAMA* **2001**, *286*, 954.
9. Mukherjee, D. *Biochem. Pharmacol.* **2002**, *63*, 817.
10. Juni, P.; Nartey, L.; Reichenbach, S.; Sterchi, R.; Dieppe, P. A.; Egger, M. *Lancet* **2004**, *364*, 2021.
11. Lichtenberger, L. M. *Biochem. Pharmacol.* **2001**, *61*, 631.
12. Tanaka, K.; Tomisato, W.; Hoshino, T.; Ishihara, T.; Namba, T.; Aburaya, M.; Katsu, T.; Suzuki, K.; Tsutsumi, S.; Mizushima, T. *J. Biol. Chem.* **2005**, *280*, 31059.
13. Tsutsumi, S.; Gotoh, T.; Tomisato, W.; Mima, S.; Hoshino, T.; Hwang, H. J.; Takenaka, H.; Tsuchiya, T.; Mori, M.; Mizushima, T. *Cell Death Differ.* **2004**, *11*, 1009.
14. Tomisato, W.; Tanaka, K.; Katsu, T.; Kakuta, H.; Sasaki, K.; Tsutsumi, S.; Hoshino, T.; Aburaya, M.; Li, D.; Tsuchiya, T.; Suzuki, K.; Yokomizo, K.; Mizushima, T. *Biochem. Biophys. Res. Commun.* **2004**, *323*, 1032.
15. Tomisato, W.; Tsutsumi, S.; Rokutan, K.; Tsuchiya, T.; Mizushima, T. *Am J. Physiol. Gastrointest. Liver Physiol.* **2001**, *281*, G1092.
16. Aburaya, M.; Tanaka, K.; Hoshino, T.; Tsutsumi, S.; Suzuki, K.; Makise, M.; Akagi, R.; Mizushima, T. *J. Biol. Chem.* **2006**, *281*, 33422.
17. Tsutsumi, S.; Namba, T.; Tanaka, K. I.; Arai, Y.; Ishihara, T.; Aburaya, M.; Mima, S.; Hoshino, T.; Mizushima, T. *Oncogene* **2006**, *25*, 1018.
18. Namba, T.; Hoshino, T.; Tanaka, K.; Tsutsumi, S.; Ishihara, T.; Mima, S.; Suzuki, K.; Ogawa, S.; Mizushima, T. *Mol. Pharmacol.* **2007**, *71*, 860.
19. Ishihara, T.; Hoshino, T.; Namba, T.; Tanaka, K.; Mizushima, T. *Biochem. Biophys. Res. Commun.* **2007**, *356*, 711.
20. Tomisato, W.; Tsutsumi, S.; Hoshino, T.; Hwang, H. J.; Mio, M.; Tsuchiya, T.; Mizushima, T. *Biochem. Pharmacol.* **2004**, *67*, 575.
21. Misaka, E.; Yamaguchi, T.; Iizuka, Y.; Kamoshida, K.; Kojima, T.; Kobayashi, K.; Endo, Y.; Misawa, Y.; Lobayashi, S.; Tanaka, K. *Pharmacometrics* **1981**, *21*, 753.
22. Kawano, S.; Tsuji, S.; Hayashi, N.; Takei, Y.; Nagano, K.; Fusamoto, H.; Kamada, T. *J. Gastroenterol. Hepatol.* **1995**, *10*, 81.
23. Sugimoto, M.; Kojima, T.; Asami, M.; Iizuka, Y.; Matsuda, K. *Biochem. Pharmacol.* **1991**, *42*, 2363.
24. Yamakawa, N.; Suemasu, S.; Kimoto, A.; Arai, Y.; Ishihara, T.; Yokomizo, K.; Okamoto, Y.; Otsuka, M.; Tanaka, K.; Mizushima, T. *Biol. Pharm. Bull.* **2010**, *33*, 398.
25. Yamakawa, N.; Suemasu, S.; Matoyama, M.; Kimoto, A.; Takeda, M.; Tanaka, K.; Ishihara, T.; Katsu, T.; Okamoto, Y.; Otsuka, M.; Mizushima, T. *J. Med. Chem.* **2010**, *53*, 7879.
26. Miyaura, N.; Suzuki, A. *Chem. Rev.* **1995**, *95*, 2457.
27. Stanforth, S. P. *Tetrahedron* **1998**, *54*, 263.
28. Kurumbail, R. G.; Stevens, A. M.; Gierse, J. K.; McDonald, J. J.; Stegeman, R. A.; Pak, J. Y.; Gildehaus, D.; Miyashiro, J. M.; Penning, T. D.; Seibert, K.; Isakson, P. C.; Stallings, W. C. *Nature* **1996**, *384*, 644.
29. Loll, P. J.; Picot, D.; Ekabo, O.; Garavito, R. M. *Biochemistry* **1996**, *35*, 7330.
30. Loll, P. J.; Picot, D.; Garavito, R. M. *Nat. Struct. Biol.* **1995**, *2*, 637.
31. Luong, C.; Miller, A.; Barnett, J.; Chow, J.; Ramesha, C.; Browner, M. F. *Nat. Struct. Biol.* **1996**, *3*, 927.
32. Mengle-Gaw, L. J.; Schwartz, B. D. *Mediators. Inflamm.* **2002**, *11*, 275.
33. Sekiguchi, M.; Shirasaka, M.; Konno, S.; Kikuchi, S. B. M. C. *Musculoskelet Disord.* **2008**, *9*, 15.
34. Anana, R.; Rao, P. N.; Chen, Q. H.; Knaus, E. E. *Bioorg. Med. Chem.* **2006**, *14*, 5259.
35. Zarghi, A.; Zebardast, T.; Hakimion, F.; Shirazi, F. H.; Rao, P. N.; Knaus, E. E. *Bioorg. Med. Chem.* **2006**, *14*, 7044.
36. Goto, J.; Kataoka, R.; Muta, H.; Hirayama, N. *J. Chem. Inf. Model.* **2008**, *48*, 583.
37. McAdam, B. F.; Catella, L. F.; Mardini, I. A.; Kapoor, S.; Lawson, J. A.; FitzGerald, G. A. *Proc. Natl. Acad. Sci. U.S.A.* **1999**, *96*, 272.
38. Catella, L. F.; McAdam, B.; Morrison, B. W.; Kapoor, S.; Kujubu, D.; Antes, L.; Lasseter, K. C.; Quan, H.; Gertz, B. J.; FitzGerald, G. A. *J. Pharmacol. Exp. Ther.* **1999**, *289*, 735.
39. Belton, O.; Byrne, D.; Kearney, D.; Leahy, A.; Fitzgerald, D. J. *Circulation* **2000**, *102*, 840.
40. Kvern, B. *Can. Fam. Physician* **2002**, *48*, 1449.
41. Esser, R.; Berry, C.; Du, Z.; Dawson, J.; Fox, A.; Fujimoto, R. A.; Haston, W.; Kimble, E. F.; Koehler, J.; Peppard, J.; Quadros, E.; Quintavalla, J.; Toscano, K.; Urban, L.; van Duzer, J.; Zhang, X.; Zhou, S.; Marshall, P. J. *Br. J. Pharmacol.* **2005**, *144*, 538.
42. Ushiyama, S.; Yamada, T.; Murakami, Y.; Kumakura, S.; Inoue, S.; Suzuki, K.; Nakao, A.; Kawara, A.; Kimura, T. *Eur. J. Pharmacol.* **2008**, *578*, 76.
43. Brideau, C.; Kargman, S.; Liu, S.; Dallob, A. L.; Ehrich, E. W.; Rodger, I. W.; Chan, C. C. *Inflamm. Res.* **1996**, *45*, 68.
44. Biddlestone, L.; Corbett, A. D.; Dolan, S. *Br. J. Pharmacol.* **2007**, *151*, 285.

British Journal of Nutrition (2011), **106**, 475–485
doi:10.1017/S0007114511000365

Protective effect of β-(1,3 → 1,6)-D-glucan against irritant-induced gastric lesions

Ken-ichiro Tanaka[1], Yuta Tanaka[1], Toshio Suzuki[2] and Tohru Mizushima[1]*

[1]*Graduate School of Medical and Pharmaceutical Sciences, Kumamoto University, 5-1 Oe-honmachi, Kumamoto 862-0973, Japan*

[2]*Research and Development, Daiso Company Limited, Amagasaki 660-0842, Japan*

(Received 17 August 2010 – Revised 18 November 2010 – Accepted 20 December 2010 – First published online 29 March 2011)

Abstract

β-(1,3)-D-Glucan with β-(1,6) branches has been reported to have various pharmacological activities, such as anti-tumour and anti-infection activities, which result from its immunomodulating effects. Gastric lesions result from an imbalance between aggressive and defensive factors. In the present study, we examined the effect of β-(1,3)-D-glucan with β-(1,6) branches isolated from *Aureobasidium pullulans* on the gastric ulcerogenic response in mice. Oral administration of β-glucan ameliorated gastric lesions induced by ethanol (EtOH) or HCl. This administration of β-glucan also suppressed EtOH-induced inflammatory responses, such as infiltration of neutrophils and expression of pro-inflammatory cytokines, chemokines and cell adhesion molecules (CAM) at the gastric mucosa. Of the various defensive factors, the levels of heat shock protein (HSP) 70 and mucin but not PGE_2 were increased by the administration of β-glucan. β-Glucan-dependent induction of the expression of HSP70 and mucin proteins and suppression of the expression of pro-inflammatory cytokines, chemokines and CAM were also observed in cultured cells *in vitro*. The results of the present study suggest that β-glucan protects the gastric mucosa from the formation of irritant-induced lesions by increasing the levels of defensive factors, such as HSP70 and mucin.

Key words: **β-(1,3 → 1,6)-D-Glucan: Gastric lesions: Heat shock protein 70: Mucin: Ethanol**

The balance between aggressive and defensive factors determines whether gastric lesions develop, with either a relative increase in aggressive factors or a relative decrease in defensive factors resulting in lesions. The gastric mucosa is challenged by a variety of both endogenous and exogenous irritants (aggressive factors), including ethanol (EtOH), gastric acid, pepsin, reactive oxygen species and non-steroidal anti-inflammatory drugs[1]. In order to protect the gastric mucosa against these aggressive factors, a complex defence system, which includes the production of surface mucus (gastric mucin) and bicarbonate and the regulation of gastric mucosal blood flow, has evolved. PG, in particular PGE_2, enhance these protective mechanisms, and are therefore thought to be a major gastric mucosal defensive factor[2].

Recently, heat shock proteins (HSP) have also attracted considerable attention as another important defensive factor. When cells are exposed to stressors, HSP are induced in a manner that is dependent on the transcription factor heat shock factor 1 (HSF1), and this cellular up-regulation, in particular the up-regulation of HSP70, provides resistance to such stressors[3–6]. We have recently reported that HSF1-null mice or transgenic mice expressing HSP70 show sensitive or resistant phenotypes, respectively, to irritant-induced gastric lesions[7,8], suggesting that HSP, especially HSP70, play an important role in the protection of the gastric mucosa against irritant-induced gastric lesions.

Chemicals that decrease the level of aggressive factors or increase the level of defensive factors are beneficial for protecting the gastric mucosa against the formation of irritant-induced lesions. Acid-control drugs, such as histamine-2 receptor antagonists and proton pump inhibitors, and anti-*Helicobacter pylori* drugs belong to the former group, while drugs that induce the production of gastric mucins, PG and HSP belong to the latter. These chemicals (anti-ulcer drugs) decrease the incidence of surgery for the treatment of gastric ulcers, resulting in a good quality of life for patients with this disease. However, in order to decrease healthcare costs and to prevent the development of gastric ulcers, it is important to find health foods and supplements (complementary and alternative medicines) that can reduce the level of aggressive factors or increase the level of defensive factors.

Abbreviations: CAM, cell adhesion molecule; EtOH, ethanol; HSF1, heat shock factor 1; HSP, heat shock protein; LMW β-glucan, low-molecular-weight β-(1,3 → 1,6)-D-glucan; MPO, myeloperoxidase.

***Corresponding author:** Dr T. Mizushima, email mizu@gpo.kumamoto-u.ac.jp

β-Glucans are naturally occurring polysaccharides found in the cell walls of yeast, fungi, cereal plants and certain bacteria[9,10]. As suggested by the fact that various foods contain β-glucans, they are known to have little toxic and adverse effects[9]. β-Glucans from fungi occur as β-(1,3)-linked glucose polymers with β-(1,6) side chains of varying length and distribution[9–11]. Such β-glucans from mushrooms have been used as anti-tumour drugs in Japan[10]. They are thought to achieve anti-tumour effects through their immunoactivating activities, such as stimulating the release of cytokines, NO and arachidonic acid metabolites[10–14]. In addition, β-(1,3)-D-glucans with β-(1,6) branches have been reported to have various other beneficial effects, such as enhancing defence against bacterial, viral, fungal and parasitic challenge, increasing haematopoiesis and radioprotection, stimulating the wound-healing response, and decreasing the levels of serum lipids[9,10,15,16]. Interestingly, it has recently been reported that β-glucans suppress inflammatory responses in some animal models by decreasing the levels of pro-inflammatory cytokines, chemokines and cell adhesion molecules (CAM)[17–22]. This suggests that β-glucan is an interesting immunomodulator, causing opposing effects on immune systems. Since the cytoprotective effects of β-glucans and suppression by β-glucans of anti-tumour drug-induced damage in the small intestine have been reported[17,23,24], it is possible that β-glucans protect against the formation of irritant-induced gastric lesions. However, no studies have examined this possibility to date.

We have used β-(1,3)-D-glucan with β-(1,6) branches isolated from *Aureobasidium pullulans*[14,25]. In general, β-(1,3)-D-glucans with β-(1,6) branches have a high molecular weight (over 2000 kDa), high viscosity and low water solubility. In addition, such β-glucans easily form gels containing high-order structures of single or triplet spirals. Therefore, its purification is extremely difficult and, in previous studies, crude β-glucan fractions rather than purified ones have been used in experiments[9]. We succeeded in the purification and industrial-scale production of low-molecular-weight β-(1,3 → 1,6)-D-glucan (LMW β-glucan) from the *A. pullulans* GM-NH-1A1 strain (black yeast, a mutant strain K-1)[14]. The characteristic features of this β-glucan are its LMW (about 100 kDa), low viscosity, high water solubility and high level of β-(1-6) branching (50–80 %)[14,25]. We have previously reported that LMW β-glucan has various clinically beneficial effects, such as suppression of the allergic response by increasing the levels of IL-12 and interferon-γ; suppression of restraint stress-induced immunosuppression (such as suppression of natural killer cell activity and IL-12 and IL-6 production); anti-tumour and anti-metastatic actions mediated via stimulation of the immune system in the small intestine; and protective effects against anti-tumour drug-induced damage in the small intestine[14,23,25,26]. In the present study, we found that LMW β-glucan protects the gastric mucosa of mice against the formation of irritant-induced lesions. We also suggest that LMW β-glucan achieves this gastroprotective effect by increasing the levels of defensive factors, such as HSP70 and gastric mucin.

Materials and methods

Chemicals and animals

LMW β-glucan was prepared from the conditioned culture medium of *A. pullulans* GM-NH-1A1, as described previously[14,25]. Analysis of ^{1}H and ^{13}C NMR spectra and gel-filtration chromatography revealed that LMW β-glucan has approximately 70 % β-(1-6) branches and an average molecular weight of 100 kDa, as described previously[14,25]. Lipopolysaccharide, U0126 (an inhibitor of extracellular signal-regulated kinase), paraformaldehyde, peroxidase standard, fetal bovine serum, *o*-dianisidine and hexadecyl trimethyl ammonium bromide were obtained from Sigma (St Louis, MO, USA). α-(1,4 → 1,6)-D-Glucan (pullulan, molecular weight 50 000–100 000) was obtained from WAKO Pure Chemicals (Tokyo, Japan). Terminal deoxynucleotidyl transferase was obtained from Toyobo (Osaka, Japan). SB203580 (an inhibitor of p38 mitogen-activated protein kinase (p38)), SP600125 (an inhibitor of c-jun NH_2-terminal kinase) and the ELISA kit for detection of PGE_2 were from Cayman Chemicals (Ann Arbor, MI, USA). Biotin 14-ATP and Alexa Fluor 488 conjugated with streptavidin were purchased from Invitrogen (Carlsbad, CA, USA). Mounting medium for immunohistochemical analysis (VECTASHIELD) was from Vector Laboratories (Burlingame, CA, USA). The RNeasy kit was obtained from Qiagen (Valencia, CA, USA), the PrimeScript® 1st strand cDNA Synthesis Kit was from TAKARA Bio (Ohtsu, Japan) and the iQ SYBR Green Supermix was from Bio-Rad (Hercules, CA, USA). Mayer's haematoxylin, 1 % eosin alcohol solution, cold Schiff's reagent, sulphate solution, 1 % periodic acid solution and mounting medium for histological examination (malinol) were from MUTO Pure Chemicals (Tokyo, Japan). The compound 4,6-diamino-2-phenylindole was from Dojindo (Kumamoto, Japan). Antibodies against HSP70 (for immunohistochemical analysis) and dectin-1 were from R&D Systems (Minneapolis, MN, USA). An antibody against HSP70 (for immunoblotting analysis) was from Stressgen (Ann Arbor, MI, USA), while one against HSF1 was kindly provided by Dr Akira Nakai (Yamaguchi University, Yoshida, Japan).

Wild-type ICR mice (6–8 weeks old, male) were used. The experiments and procedures described here were carried out in accordance with the Guide for the Care and Use of Laboratory Animals as adopted and promulgated by the National Institute of Health, and were approved by the Animal Care Committee of Kumamoto University (Kumamoto, Japan).

Gastric damage assay

Gastric ulcerogenic response was examined as described previously[7]. Mice, which had been fasted for 18 h, were orally administered either EtOH or HCl (5 ml/kg). After 4 h, the animals were killed with an overdose of diethyl ether, after which their stomachs were removed and scored for haemorrhagic damage by an observer unaware of the treatment they had received. Calculation of the scores involved measuring the area of all lesions in millimetres squared and summing the values to give an overall gastric lesion index. Gastric mucosal PGE_2 levels were determined by ELISA, as described previously[27].

Histopathological and immunohistochemical analyses and terminal deoxynucleotidyl transferase dUTP nick-end labelling assay

Gastric tissue samples were fixed in 4% buffered paraformaldehyde, and then embedded in paraffin before being cut into 4 μm-thick sections.

For histopathological examination, sections were stained first with Mayer's haematoxylin and then with 1% eosin alcohol solution (haematoxylin and eosin staining). Samples were mounted with malinol and inspected with the aid of an Olympus BX51 microscope (Tokyo, Japan).

For immunohistochemical analysis, sections were incubated with 0·3% H_2O_2 in methanol for the removal of endogenous peroxidase. Sections were blocked with 2·5% goat serum for 10 min, incubated for 12 h with an antibody against HSP70 (1:40 dilution) in the presence of 2·5% bovine serum albumin and then incubated for 2 h with a peroxidase-labelled polymer conjugated to goat anti-mouse Ig. Then, 3,3′-diaminobenzidine was applied to the sections, and the sections were finally incubated with Mayer's haematoxylin. Samples were mounted with malinol and inspected using a fluorescence microscope (Olympus BX51).

For the terminal deoxynucleotidyl transferase dUTP nick-end labelling assay, sections were incubated first with proteinase K (20 μg/ml) for 15 min at 37°C, then with TdTase and biotin 14-ATP for 1 h at 37°C and finally with Alexa Fluor 488 conjugated with streptavidin and 4,6-diamino-2-phenylindole for 2 h. Samples were mounted with VECTASHIELD and inspected with the aid of a fluorescence microscope (Olympus BX51).

Periodic acid Schiff staining

Gastric tissue samples were fixed in Carnoy's fluid (EtOH–acetic anhydride 3:1), and embedded in paraffin before being cut into 4 μm-thick sections. Sections were incubated with 1% periodic acid solution for 10 min, then with cold Schiff's reagent for 15 min and finally with sulphate solution for 2 min. Sections were incubated with Mayer's haematoxylin, mounted with malinol and inspected using a fluorescence microscope (Olympus BX51).

Real-time RT-PCR analysis

Real-time RT-PCR was performed as described previously[28], with some modifications. Total RNA was extracted using an RNeasy kit according to the manufacturer's protocol. Samples (2·5 μg RNA) were reverse-transcribed using the PrimeScript® 1st strand cDNA Synthesis Kit. Synthesised complementary DNA was used in real-time RT-PCR (Chromo 4 instrument; Bio-Rad) experiments using the iQ SYBR GREEN Supermix, and analysed with Opticon Monitor Software (Bio-Rad). Specificity was confirmed by electrophoretic analysis of the reaction products and by inclusion of template- or RT-free controls. To normalise the amount of total RNA present in each reaction, *gapdh* or *actin* complementary DNA was used as an internal standard.

Primers were designed using the Primer3 website. The primers used were as follows (name: forward primer, reverse primer). For humans, *muc-1*: 5′-acacaaacccagcagtggc-3′, 5′-actcagctcagcggcgac-3′; *muc-5ac*: 5′-cagccacgtccccttcaata-3′, 5′-accgcatttgggcatcc-3′; *actin*: 5′-ggacttcgagcaagagatgg-3′, 5′-agcactgtgttggcgtacag-3′. For mice, *tnf-α*: 5′-cgtcagccgatttgctatct-3′, 5′-cggactccgcaaagtctaag-3′; *il-1β*: 5′-gatcccaagcaatacccaaa-3′, 5′-ggggaactctgcagactcaa-3′; *il-6*: 5′-ctggagtcacagaaggagtgg-3′, 5′-ggtttgccgagtagatctcaa-3′; macrophage inflammatory protein (*mip*)-*2α*: 5′-accctgccaagggttgacttc-3′, 5′-ggcacatcaggtacgatccag-3′; monocyte chemoattractant protein (*mcp*)-*1*: 5′-ctcacctgctgctactcattc-3′, 5′-gcttgaggtggttgtggaaaa-3′; vascular cell adhesion molecule (*vcam*)-*1*: 5′-ctcctgcacttgtggaaatg-3′, 5′-tgtacgagccatccacagac-3′; intercellular adhesion molecule (*icam*)-*1*: 5′-tcgtgatggcagcctcttat-3′, 5′-gggcttgtcccttgagtttt-3′; *muc-1*: 5′-gccttcagtgccaagtcaat-3′, 5′-gaaggagaccccaacagaca-3′; *muc-5ac*: 5′-aaagacaccagtagtcactcagcaa-3′, 5′-ctgggaagtcagtgtcaaacca-3′; *gapdh*: 5′-aactttggcattgtggaagg-3′, 5′-acacattgggggtaggaaca-3′.

Myeloperoxidase activity

Myeloperoxidase (MPO) activity in the gastric tissues was measured as described previously[29,30]. Animals were placed under deep diethyl ether anaesthesia and killed. Stomachs were dissected, rinsed with cold saline and cut into small pieces. Samples were homogenised, freeze-thawed and centrifuged. The protein concentrations of the supernatants were determined using the Bradford method[31]. MPO activity was determined in 10 mM-phosphate buffer with 0·5 mM-*o*-dianidisine, 0·00 005% (w/v) H_2O_2 and 20 μg protein. MPO activity was obtained from the slope of the reaction curve, and its specific activity was expressed as the number of H_2O_2 molecules converted/min per mg protein.

Preparation of mouse peritoneal macrophages

Mouse peritoneal macrophages were prepared as described previously[32]. Mice were given 2 ml of 10% proteose peptone by intraperitoneal injection and peritoneal cells were harvested 3 d later. The cells were seeded in 60 mm culture dishes. After incubation for 4 h, non-adherent cells were removed and the adherent cells were cultured for use in the experiments. Virtually, all of the adherent cells were macrophages, as described previously[33].

Cell culture and immunoblotting analysis

Human gastric carcinoma cells were cultured in RPMI-1640 medium supplemented with 10% fetal bovine serum, penicillin (100 μg/ml) and streptomycin (100 μg/ml) in a humidified atmosphere of 95% air with 5% CO_2 at 37°C.

Whole-cell extracts were prepared as described previously[34]. The protein concentration of the samples was determined by the Bradford method[31]. Samples were applied to polyacrylamide SDS gels and subjected to electrophoresis, and the resultant proteins were immunoblotted with an antibody for HSP70 or actin.

British Journal of Nutrition

Statistical analysis

All values are expressed as means with their standard errors. Two-way ANOVA followed by the Tukey test or Student's *t* test for unpaired results was used to evaluate differences between more than three groups or between two groups, respectively. Differences were considered to be significant for values of $P<0{\cdot}05$.

Results

Effect of low-molecular-weight β-(1,3 → 1,6)-D-glucan on gastric ulcerogenic and inflammatory responses

The effect of oral pre-administration of LMW β-glucan on the development of gastric lesions following oral administration of EtOH was examined in mice. We have previously reported

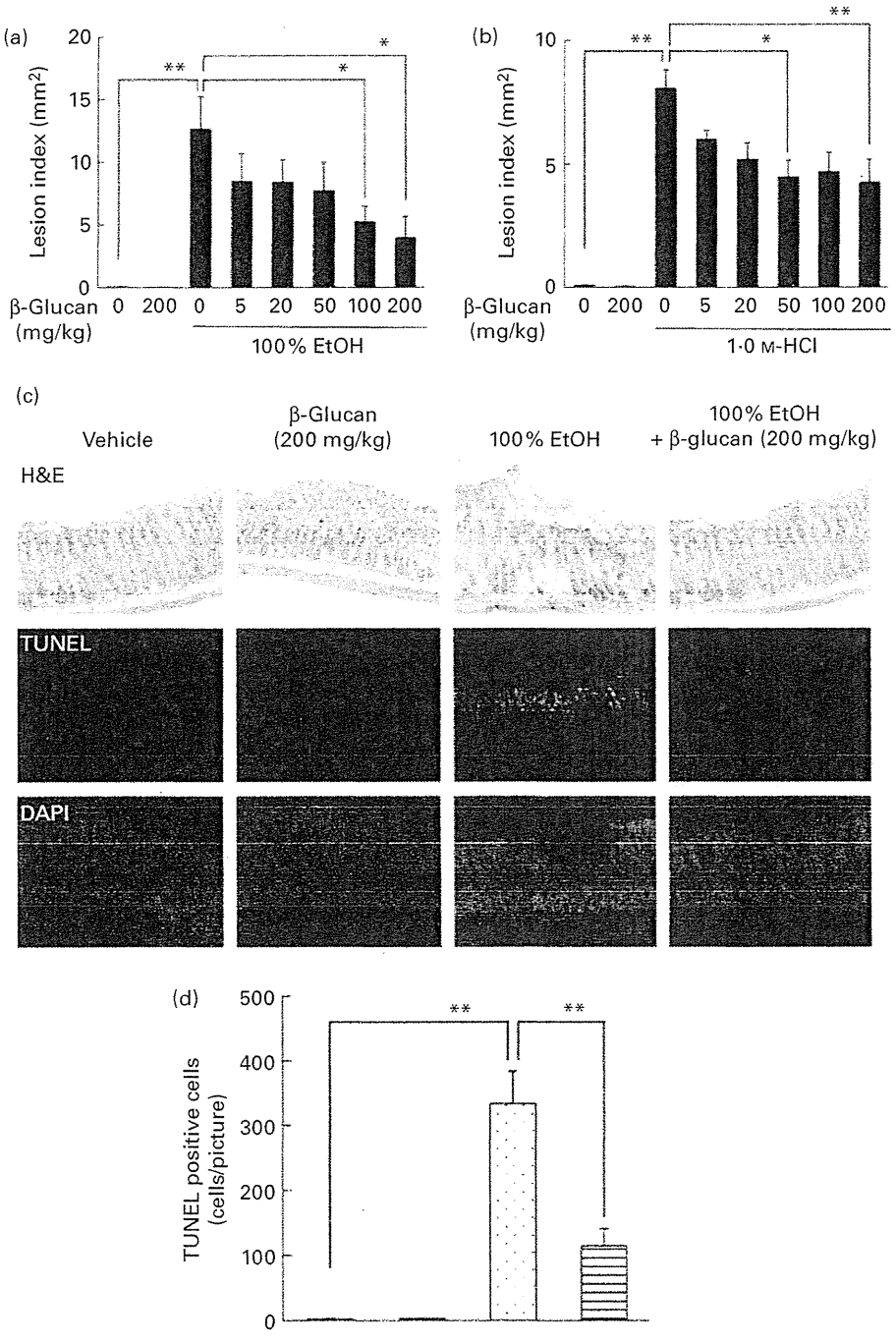

Fig. 1. Effect of low-molecular-weight β-glucan on irritant-induced gastric lesions. Mice were orally administered the indicated doses of β-glucan (mg/kg) or vehicle (□, PBS), 1 h after which they were orally administered (a, c) 100% ethanol (EtOH) (▨), (b) 1·0 M-HCl (5 ml/kg) or vehicle (water). (a, b) After 4 h, the stomach was removed and scored for haemorrhagic damage. (c) Sections of gastric tissue were prepared after 4 h and subjected to histopathological examination (haematoxylin and eosin (H&E) staining), terminal deoxynucleotidyl transferase dUTP nick-end labelling (TUNEL) assay and 4,6-diamino-2-phenylindole (DAPI) staining. (d) TUNEL-positive cells in the three sections were counted. Values are means, with their standard errors represented by vertical bars (n 3–17). Mean values were significantly different: * $P<0{\cdot}05$, ** $P<0{\cdot}01$. ■, β-Glucan (200 mg/kg); ▤, 100% EtOH + β-glucan (200 mg/kg).

British Journal of Nutrition

that oral administration of EtOH induces the expression of HSP70 in a HSF1-dependent manner, and this induction is accompanied by the production of gastric lesions[7]. As shown in Fig. 1(a), intragastric administration of 100% EtOH resulted in significant gastric lesion formation and oral pre-administration of LMW β-glucan suppressed this production in a dose-dependent manner. Oral administration of LMW β-glucan (200 mg/kg) alone did not produce gastric lesions (Fig. 1(a)). A similar protective effect of LMW β-glucan was observed for HCl-induced gastric lesions (Fig. 1(b)). Therefore, the protective effects of LMW β-glucan do not appear to be mediated in response to a specific stressor, such as EtOH. Histopathological examination by haematoxylin and eosin staining supports the notion that pre-administration of LMW β-glucan protects the gastric mucosa against EtOH-induced damage (Fig. 1(c)). Also, the level of gastric mucosal apoptosis was determined by the terminal deoxynucleotidyl transferase dUTP nick-end labelling assay. An increase in the number of terminal deoxynucleotidyl transferase dUTP nick-end labelling-positive (apoptotic) cells was observed following the administration of EtOH, and this increase was suppressed by pre-administration of LMW β-glucan (Fig. 1(c) and (d)). The results in Fig. 1 suggest that LMW β-glucan protects the gastric mucosa against irritant-induced lesions through the suppression of mucosal cell apoptosis.

Inflammatory responses, such as the infiltration of leucocytes, play an important role in the production of irritant-induced gastric lesions. In the present study, we examined the effect of LMW β-glucan on the EtOH-induced gastric

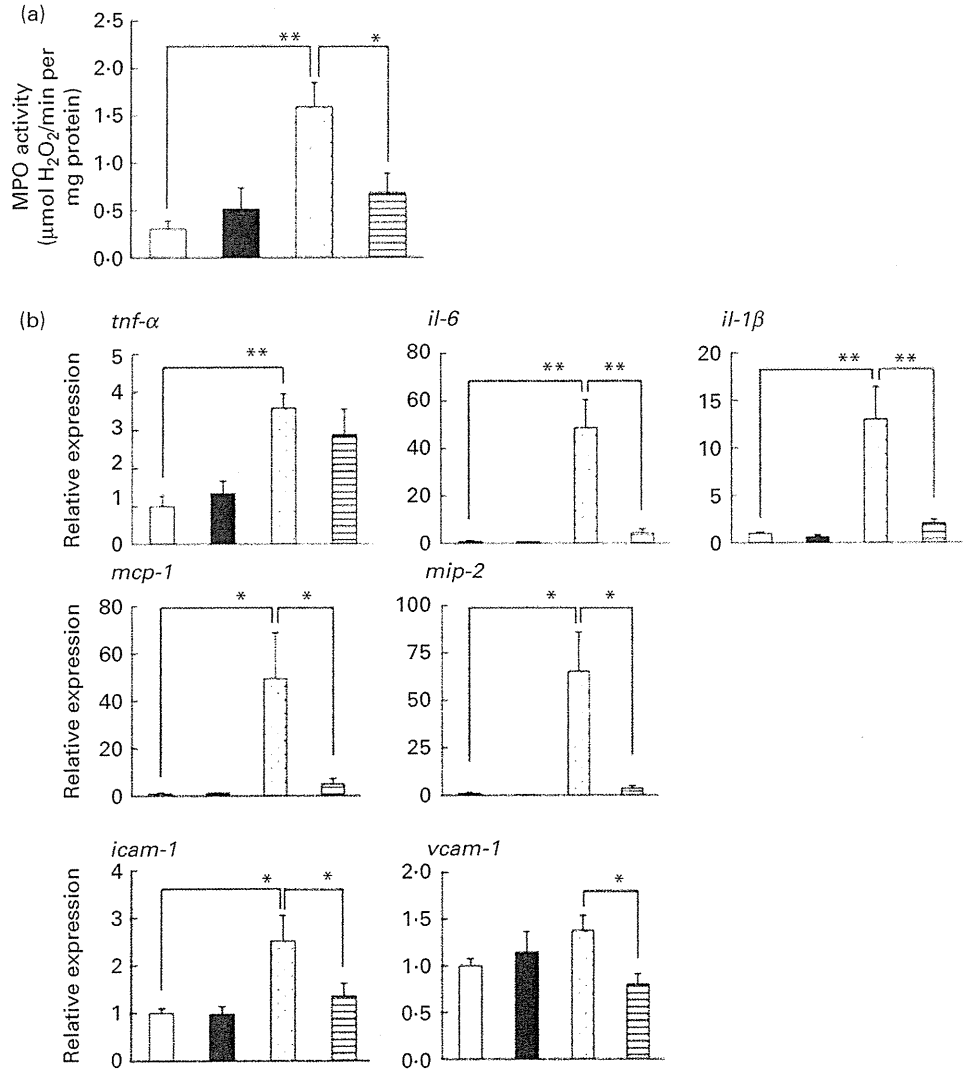

Fig. 2. Effect of low-molecular-weight β-glucan on the ethanol (EtOH)-induced gastric inflammatory response. Mice were orally administered β-glucan (■, 200 mg/kg) or vehicle (□, PBS), 1 h after which they were orally administered 100% EtOH (▤, 5 ml/kg) or vehicle (water). (a, b) After 4 h, the stomach was removed. (a) Gastric myeloperoxidase (MPO) activity was determined as described in the Materials and methods. Total RNA was extracted and subjected to real-time RT-PCR using a specific primer set for each gene. (b) Values were normalised to the *gapdh* gene and expressed relative to the control sample. Values are means, with their standard errors represented by vertical bars (n 9–14). Mean values were significantly different: * $P<0·05$, ** $P<0·01$. ▤, 100% EtOH + β-glucan (200 mg/kg). *mcp-1*, Monocyte chemoattractant protein-1; *mip-2*, macrophage inflammatory protein-2; *icam-1*, intercellular adhesion molecule-1; *vcam-1*, vascular cell adhesion molecule-1.

immunoblotting analysis. As shown in Fig. 3(a) and (b), either LMW β-glucan or EtOH significantly induced the expression of HSP70. Immunohistochemical analysis supported the notions that either LMW β-glucan or EtOH induced the expression of HSP70 (Fig. 3(c)).

We also examined by periodic acid Schiff staining the effect of LMW β-glucan and/or EtOH on the level of gastric mucin. As shown in Fig. 3(d), the level of gastric mucin was reduced by the administration of EtOH, and pre-administration of LMW β-glucan restored the level. We also examined the mRNA expression of representative gastric mucin genes (*muc-1* and *muc-5ac*)[35] by real-time RT-PCR. Muc1 is a membrane-bound protein and Muc-5ac is a secreted protein[36]. As shown in Fig. 3(e), the expression of *muc-1* and *muc-5ac* mRNA was suppressed by the administration of EtOH and pre-administration of LMW β-glucan restored the expression.

The effect of LMW β-glucan and/or EtOH on gastric PGE_2 levels was also studied. As shown in Fig. 3(f), neither LMW β-glucan nor EtOH administration affected the level of PGE_2. The results in Fig. 3 suggest that LMW β-glucan protects the gastric mucosa against EtOH-induced lesions by increasing the levels of HSP70 and gastric mucin rather than that of PGE_2.

Effect of low-molecular-weight β-(1,3 → 1,6)-D-glucan on the expression of genes in vitro

In order to test whether LMW β-glucan directly affects the expression of HSP70 and mucin proteins, we examined its effect on the expression of these factors in cultured human gastric carcinoma cells. Immunoblotting analysis revealed that treatment of cells with LMW β-glucan significantly induces the expression of HSP70 in a dose-dependent manner (Fig. 4(a) and (b)).

We then examined the molecular mechanism for the LMW β-glucan-induced expression of HSP70. It is known that stressor-induced expression of HSP is mediated by the activation (phosphorylation) of HSF1. As shown in Fig. 4(c), as well as heat treatment, treatment of cells with LMW β-glucan increased the level of phosphorylated HSF1, suggesting that LMW β-glucan activates HSF1.

Previous studies have suggested that mitogen-activated protein kinases, such as p38, extracellular signal-regulated kinase and c-jun NH_2-terminal kinase, are involved in the regulation of the expression of HSP[37,38]. Therefore, we here examined the effect of inhibitors of mitogen-activated protein kinase on the LMW β-glucan-induced expression of HSP70. Pretreatment

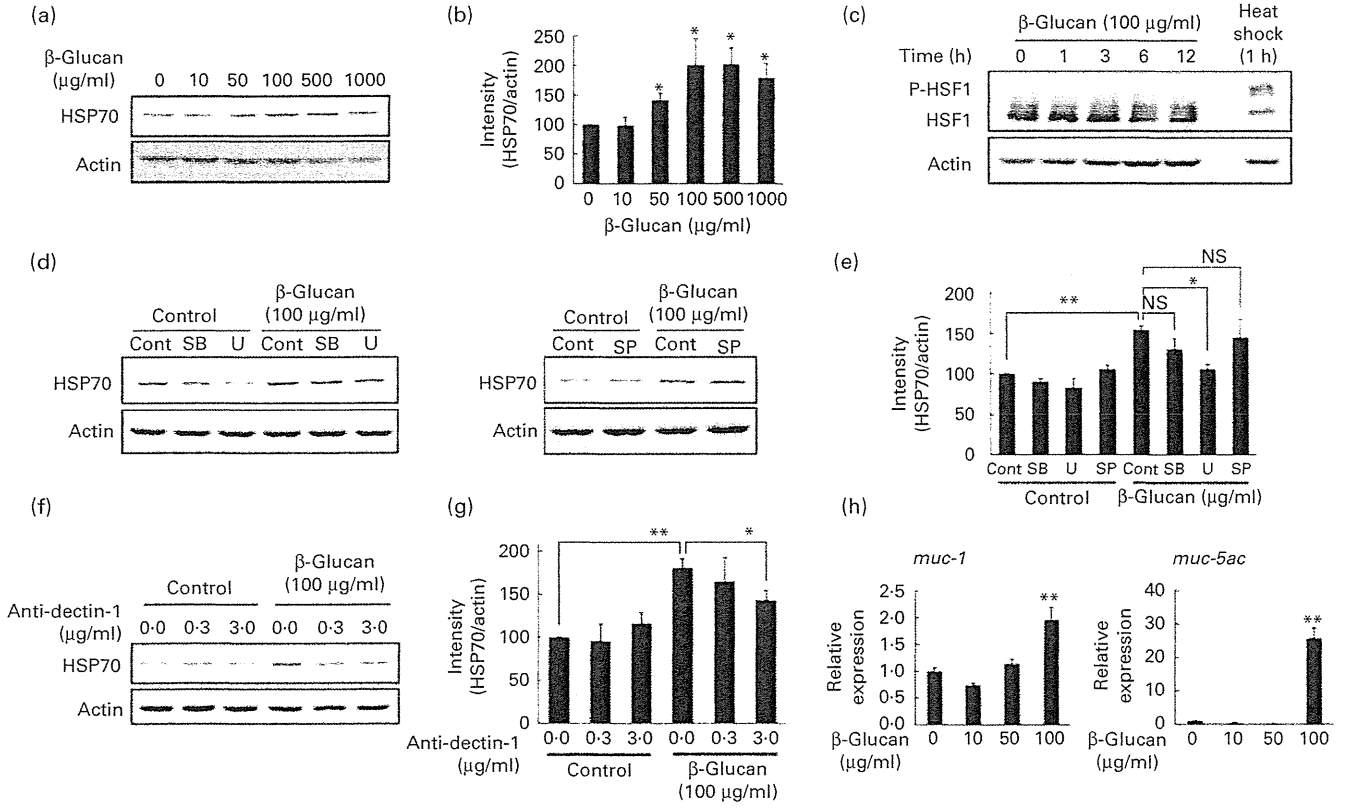

Fig. 4. Effect of low-molecular-weight (LMW) β-glucan on the expression of heat shock protein (HSP) 70 and mucin genes *in vitro*. (d, f) Human gastric carcinoma cells were pre-incubated for 1 h with or without 10 μM-SB203580 (SB), 10 μM-U0126 (U), 10 μM-SP600125 (SP) or indicated concentrations of an antibody against dectin-1. Cells were incubated with (a, h) the indicated concentrations or (c, d, f) 100 μg/ml of LMW β-glucan for (a, d, f, h) 24 h or (c) indicated periods. (c) Cells were cultured at 42°C for 1 h (heat shock). Total proteins were analysed by immunoblotting with an antibody against HSP70, heat shock factor 1 (HSF1) or actin ((a), (c), (d), (f)) (P-HSF1, phosphorylated form of HSF1). (b, e, g) The relative intensity of the HSP70 band to the actin band is shown (one of the gels is shown in (a, d, f)). The expression of mucin (*muc*)-*1* or *muc-5ac* mRNA was monitored by real-time RT-PCR, as described in the legend of Fig. 2. (h) Values were normalised to the *actin* gene. Values are means, with their standard errors represented by vertical bars (n 3–6). Mean values were significantly different: * $P<0·05$, ** $P<0·01$. cont, Control.

British Journal of Nutrition

of cells with U0126 but not with SB203580 or SP600125 partially suppressed the LMW β-glucan-induced expression of HSP70 (Fig. 4(d) and (e)), suggesting that extracellular signal-regulated kinase is involved in the LMW β-glucan-induced expression of HSP70.

Dectin-1 was reported to be a receptor for β-glucan. In order to test the involvement of dectin-1, we examined the effect of addition of antibody against dectin-1 in the culture medium on the LMW β-glucan-induced expression of HSP70. As shown in Fig. 4(f) and (g), addition of antibody against dectin-1 in the culture medium partially suppressed the β-glucan-induced expression of HSP70, suggesting that dectin-1 is involved in the LMW β-glucan-induced expression of HSP70.

Real-time RT-PCR analysis revealed that treatment of cells with LMW β-glucan induces the expression of *muc-1* and *muc-5ac* mRNA (Fig. 4(h)).

We also examined the effect of LMW β-glucan on the lipopolysaccharide-stimulated expression of pro-inflammatory cytokines, chemokines and CAM in peritoneal macrophages prepared from mice. As shown in Fig. 5, lipopolysaccharide stimulated the mRNA expression of all these factors, and the simultaneous treatment of cells with LMW β-glucan suppressed this lipopolysaccharide-stimulated expression. The results in Figs. 4 and 5 suggest that LMW β-glucan directly affects the expression of HSP70, mucin proteins, pro-inflammatory cytokines, chemokines and CAM.

Effect of pullulan on gastric ulcerogenic response and the expression of heat shock protein 70

Since we used relatively high doses of LMW β-glucan, it may non-specifically interact with the irritants and protect the gastric mucosa. Thus, in order to test the specificity, we used another polysaccharide (α-(1,4 → 1,6)-D-glucan (pullulan)) with molecular weight similar to LMW β-glucan as the control. As shown in Fig. 6(a), oral pre-administration of pullulan (up to 200 mg/kg) did not protect the gastric mucosa against EtOH. We also examined the effect of pullulan on the expression of HSP70 both *in vivo* and *in vitro*. Oral administration of pullulan (200 mg/kg) did not increase the expression of HSP70 at the gastric mucosa with and without simultaneous administration of EtOH (Fig. 6(b) and (c)). Furthermore, treatment of human gastric carcinoma cells with pullulan (up to 1 mg/ml) did not affect the expression of HSP70 (Fig. 6(d)). Results in Fig. 6 suggest that LMW β-glucan specifically protects the gastric mucosa against irritants and induces the expression of HSP70.

Discussion

β-Glucans have been reported to have various clinically beneficial effects, such as anti-tumour effects and protective effects against bacterial, viral, fungal and parasitic challenge[9,10].

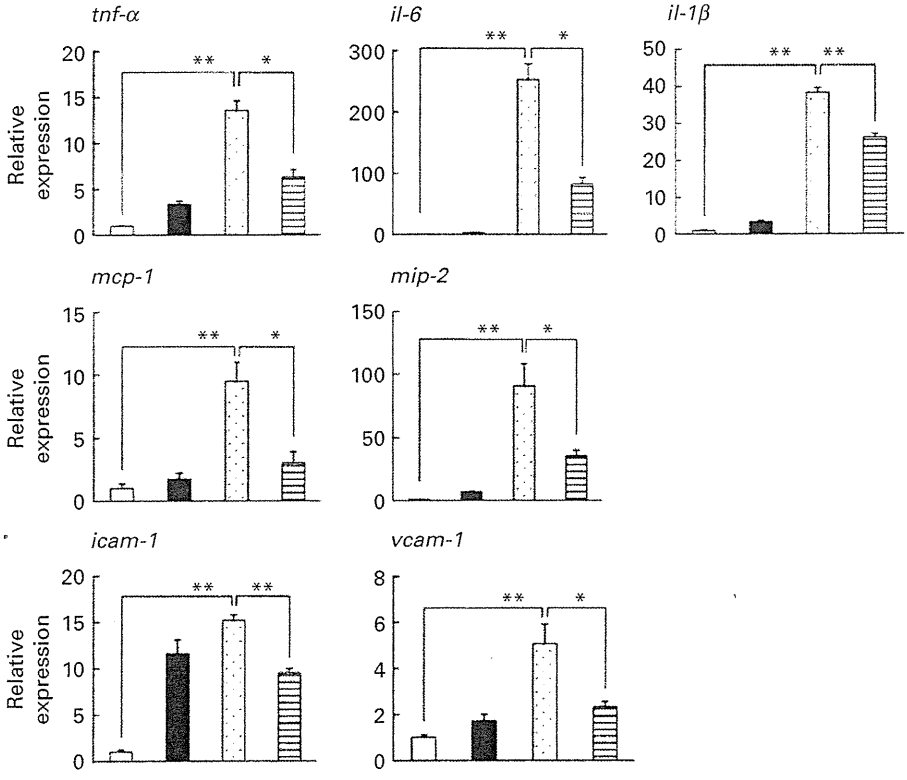

Fig. 5. Effect of low-molecular-weight β-glucan on the lipopolysaccharide (LPS)-stimulated expression of pro-inflammatory cytokines in cultured macrophages. Peritoneal macrophages were pre-incubated with β-glucan (■, 100 μg/ml) for 1 h and further incubated with LPS (▤, 1 μg/ml) for 3 h in the presence of β-glucan (100 μg/ml) as in the pre-incubation step. The expression of genes was monitored by real-time RT-PCR as described in the legend of Fig. 4. Values are means, with their standard errors represented by vertical bars (n 3–6). Mean values were significantly different: * $P<0.05$; ** $P<0.01$. □, Vehicle; ▤, LPS (1 μg/ml) + β-glucan (100 μg/ml). *mcp-1*, Monocyte chemoattractant protein-1; *mip-2*, macrophage inflammatory protein-2; *icam-1*, intercellular adhesion molecule-1; *vcam-1*, vascular cell adhesion molecule-1.

British Journal of Nutrition

inflammatory response by measuring gastric MPO activity, an indicator of inflammatory infiltration of neutrophils. As shown in Fig. 2(a), MPO activity increased in response to the administration of EtOH, and this increase was suppressed by pre-administration of LMW β-glucan. The administration of LMW β-glucan alone did not significantly affect the MPO activity (Fig. 2(a)).

We also examined the effects of LMW β-glucan and/or EtOH on the mRNA expression of pro-inflammatory cytokines (IL-6, IL-1β and TNF-α), chemokines (MCP-1 and MIP-2) and CAM (ICAM-1 and VCAM-1) by real-time RT-PCR analysis. As shown in Fig. 2(b), mRNA expression of all these genes except *vcam-1* was induced by EtOH administration, and this induction of the expression of all these genes except *tnf-α* was suppressed by pre-administration of LMW β-glucan. These results suggest that LMW β-glucan suppresses gastric inflammatory responses by suppressing the expression of pro-inflammatory cytokines, chemokines and CAM.

Effect of low-molecular-weight β-(1,3 → 1,6)-D-glucan on defensive factors for the gastric mucosa

In order to understand the molecular mechanism governing the protective effect of LMW β-glucan on the gastric mucosa, we examined its effect on various gastric mucosal defensive factors, such as HSP70, mucin proteins and PGE_2 *in vivo*. First, we examined the effect of LMW β-glucan and/or EtOH on HSP70 expression at the gastric mucosa by

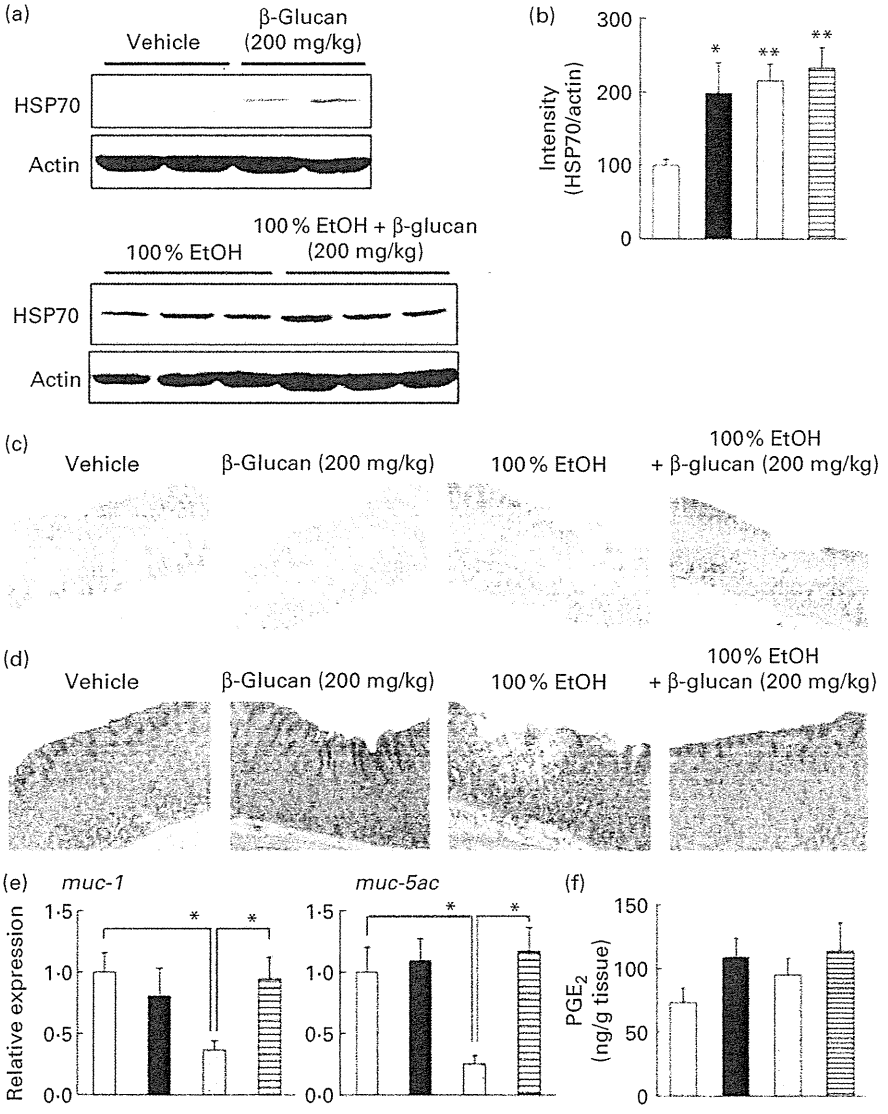

Fig. 3. Effect of low-molecular-weight β-glucan on the defensive factors for the gastric mucosa. Administration of β-glucan (■, 200 mg/kg) and 100% ethanol (EtOH, ▨) was performed as described in the legend of Fig. 2. After 4 h, the stomach was removed. (a) Total proteins were analysed by immunoblotting with an antibody against heat shock protein (HSP) 70 or actin. (b) The relative intensity of the HSP70 band to the actin band is shown (one of the gels is shown in (a)). Sections of gastric tissue were prepared and subjected to immunohistochemical analysis with an antibody against (c) HSP70 or (d) periodic acid Schiff staining. (e) The expression of mucin (*muc*)-*1* or *muc-5ac* mRNA was monitored by real-time RT-PCR, as described in the legend of Fig. 2. (f) The gastric PGE_2 level was determined by ELISA. Values are means, with their standard errors represented by vertical bars (n 3–9). Mean values were significantly different: * $P<0·05$, ** $P<0·01$. □, Vehicle; ▤, 100% EtOH + β-glucan (200 mg/kg).

Of the β-glucans, our preparation of β-(1,3)-D-glucan with β-(1,6) branches from *A. pullulans* (LMW β-glucan) is characterised by a LMW, high purity, high water solubility, low viscosity and a high level of β-(1-6) branching[14,25]. It has also been shown to have various clinically beneficial effects such as suppression of the allergic response and anti-tumour and anti-metastatic actions[14,23,25,26]. In the present study, we found another beneficial effect of LMW β-glucan, a protective effect against the formation of irritant-induced gastric lesions. Because β-glucans are known to have minimal toxic and adverse effects, we propose that β-glucans, especially LMW β-glucan, may be beneficial as health foods and supplements to prevent the formation of gastric ulcers. The findings in the present study are also important from the nutritional standpoint. Various foods, such as mushrooms, contain β-glucans. Results in the present study suggest that the intake of such foods spontaneously protects our gastric mucosa against the production of gastric lesions. Due to technical problem, we could not examine the pharmacokinetics of LMW β-glucan (such as digestion and absorption). As for other β-glucans, it has been reported that the bioavailability is from 0·5 to 5% upon oral administration[39].

Both gastric mucosal apoptosis and inflammatory responses (such as infiltration of leucocytes) play an important role in the production of irritant-induced gastric lesions, and in the present study, we have shown that both these responses are suppressed by the administration of LMW β-glucan. The anti-apoptotic effect of β-glucans has also been reported elsewhere[17,24]. On the other hand, as described earlier, β-glucans have been reported to show opposing (positive or negative) effects on immunoreactions, including inflammation. Possible explanations for this discrepancy include differences in the administration route, average molecular weight, water solubility and purity of the β-glucans employed. Another explanation is that β-glucans may have positive or negative effects on immunoreactions depending on the experimental conditions. In previous reports and in the present study, β-glucans were shown to suppress immunoreactions when the reactions were initiated by other stimuli[17–22]. On the other hand, β-glucans activate immunoreactions in intact animals[9,10,11,13]. We consider that β-glucan is a unique immunomodulator, suppressing immunoreactions when they are abnormally activated, and activating immunoreactions under normal conditions, which is important for maintaining healthy conditions.

Of the three major defensive factors for the gastric mucosa (HSP70, gastric mucin and PGE_2), we found that gastric levels of HSP70 and mucin were increased by LMW β-glucan, suggesting that these increases are responsible for the protective effect of LMW β-glucan against the formation of irritant-induced gastric lesions. We also found that EtOH-induced expression of pro-inflammatory cytokines, chemokines and CAM was suppressed by LMW β-glucan. In addition to its cytoprotective effects, the anti-inflammatory activity of HSP70 has recently been revealed; HSP70 inhibits NF-κB, which induces the expression of pro-inflammatory cytokines, chemokines and CAM[40,41]. Thus, LMW β-glucan-induced expression of HSP70 may be involved in its inhibitory

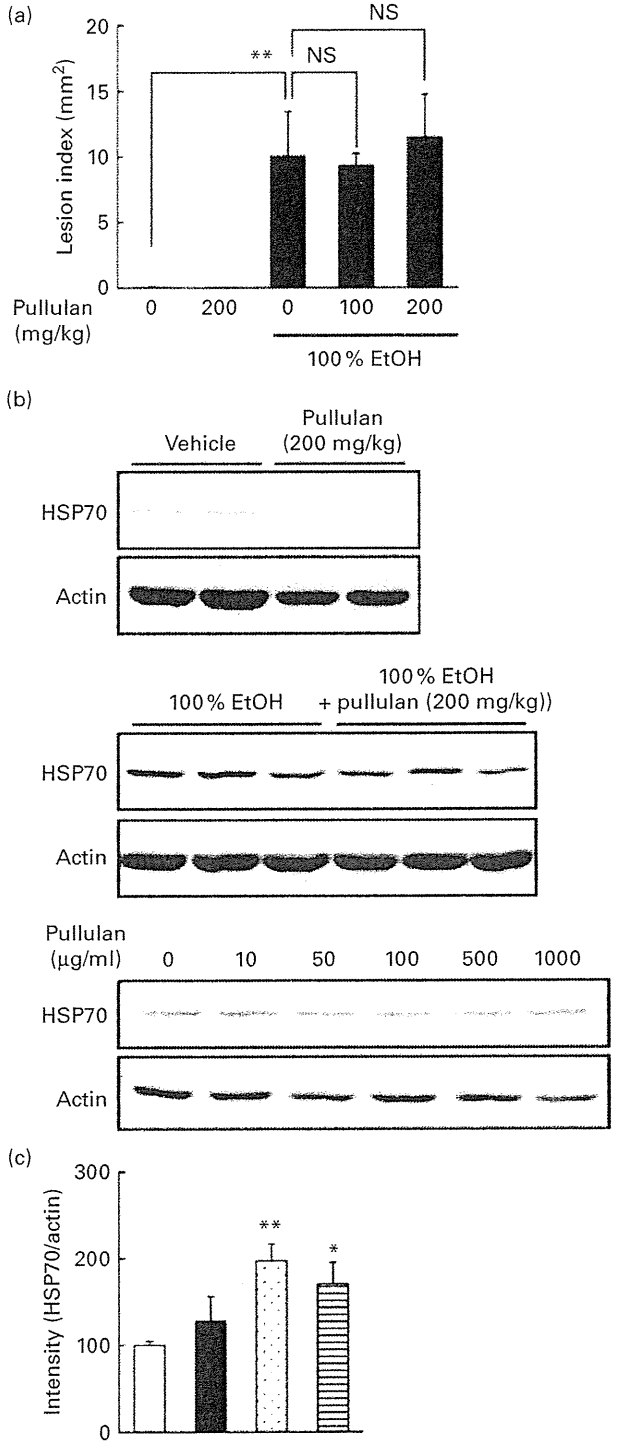

Fig. 6. Effect of pullulan on irritant-induced gastric lesions. The effect of the oral administration of pullulan on (a) ethanol (EtOH)-induced gastric lesions and (b, c) EtOH-induced expression of heat shock protein (HSP) 70 was examined as described in the legend of Figs. 1 and 3, respectively. (d) The effect of pullulan on the EtOH-induced expression of HSP70 in human gastric carcinoma cells was examined as described in the legend of Fig. 4. Values are means, with their standard errors represented by vertical bars (n 3–5). Mean values were significantly different: * $P<0·05$, ** $P<0·01$. □, Vehicle; ■, pullulan (200 mg/kg); ▦, 100% EtOH; ▤, 100% EtOH + pullulan (200 mg/kg).

British Journal of Nutrition

effects on gastric mucosal apoptosis and the inflammatory responses.

An ameliorative effect of HSP70 due to its cytoprotective, anti-inflammatory and molecular chaperone (quality control of proteins) properties has been reported for various diseases. For example, we have shown using transgenic mice expressing HSP70 that HSP70 protects against irritant-induced lesions in the stomach and small intestine, inflammatory bowel disease-related experimental colitis and UV-induced epidermal damage[7,8,30,42,43]. The potential therapeutic applicability of HSP70 for use in other diseases, such as neurodegenerative diseases, ischaemia–reperfusion damage and diabetes, has also been suggested[44–46]. Interestingly, geranylgeranylacetone, a leading anti-ulcer drug on the Japanese market, has been reported to be an HSP inducer, up-regulating various HSP not only in cultured gastric mucosal cells but also in various tissues *in vivo*[6]. It has been reported that geranylgeranylacetone suppresses not only gastric lesions but also lesions of the small intestine, inflammatory bowel disease-related experimental colitis and neurodegenerative diseases[8,42,47,48]. Therefore, the results of the present study suggest that LMW β-glucan may be beneficial not only for inhibiting the development of gastric lesions but also for the treatment of other diseases through the induction of HSP70 expression.

Acknowledgements

The present study was supported by Grants-in-Aid for Scientific Research from the Ministry of Health, Labour and Welfare of Japan, as well as the Japan Science and Technology Agency and Grants-in-Aid for Scientific Research from the Ministry of Education, Culture, Sports, Science and Technology, Japan. K.-i. T. and Y. T. did some of the experiments. T. S. prepared LMW β-glucan and T. M. is responsible for conducting the study. None of the authors has a financial relationship with a commercial entity that has an interest in the subject of the study.

References

1. Holzer P (1998) Neural emergency system in the stomach. *Gastroenterology* **114**, 823–839.
2. Miller TA (1983) Protective effects of prostaglandins against gastric mucosal damage: current knowledge and proposed mechanisms. *Am J Physiol* **245**, G601–G623.
3. Mathew A & Morimoto RI (1998) Role of the heat-shock response in the life and death of proteins. *Ann N Y Acad Sci* **851**, 99–111.
4. Gething MJ & Sambrook J (1992) Protein folding in the cell. *Nature* **355**, 33–45.
5. Kiang JG & Tsokos GC (1998) Heat shock protein 70 kDa: molecular biology, biochemistry, and physiology. *Pharmacol Ther* **80**, 183–201.
6. Hirakawa T, Rokutan K, Nikawa T, *et al.* (1996) Geranylgeranylacetone induces heat shock proteins in cultured guinea pig gastric mucosal cells and rat gastric mucosa. *Gastroenterology* **111**, 345–357.
7. Tanaka K, Tsutsumi S, Arai Y, *et al.* (2007) Genetic evidence for a protective role of heat shock factor 1 against irritant-induced gastric lesions. *Mol Pharmacol* **71**, 985–993.
8. Suemasu S, Tanaka K, Namba T, *et al.* (2009) A role for HSP70 in protecting against indomethacin-induced gastric lesions. *J Biol Chem* **284**, 19705–19715.
9. Tsoni SV & Brown GD (2008) beta-Glucans and dectin-1. *Ann N Y Acad Sci* **1143**, 45–60.
10. Chen J & Seviour R (2007) Medicinal importance of fungal beta-(1 → 3), (1 → 6)-glucans. *Mycol Res* **111**, 635–652.
11. Brown GD & Gordon S (2003) Fungal beta-glucans and mammalian immunity. *Immunity* **19**, 311–315.
12. Hashimoto T, Ohno N, Adachi Y, *et al.* (1997) Enhanced production of inducible nitric oxide synthase by beta-glucans in mice. *FEMS Immunol Med Microbiol* **19**, 131–135.
13. Engstad CS, Engstad RE, Olsen JO, *et al.* (2002) The effect of soluble beta-1,3-glucan and lipopolysaccharide on cytokine production and coagulation activation in whole blood. *Int Immunopharmacol* **2**, 1585–1597.
14. Kimura Y, Sumiyoshi M, Suzuki T, *et al.* (2006) Antitumor and antimetastatic activity of a novel water-soluble low molecular weight beta-1, 3-D-glucan (branch beta-1,6) isolated from *Aureobasidium pullulans* 1A1 strain black yeast. *Anticancer Res* **26**, 4131–4141.
15. Berdal M, Appelbom HI, Eikrem JH, *et al.* (2007) Aminated beta-1,3-D-glucan improves wound healing in diabetic db/db mice. *Wound Repair Regen* **15**, 825–832.
16. Bell S, Goldman VM, Bistrian BR, *et al.* (1999) Effect of beta-glucan from oats and yeast on serum lipids. *Crit Rev Food Sci Nutr* **39**, 189–202.
17. Sener G, Eksioglu-Demiralp E, Cetiner M, *et al.* (2006) Beta-glucan ameliorates methotrexate-induced oxidative organ injury via its antioxidant and immunomodulatory effects. *Eur J Pharmacol* **542**, 170–178.
18. Bedirli A, Kerem M, Pasaoglu H, *et al.* (2007) Beta-glucan attenuates inflammatory cytokine release and prevents acute lung injury in an experimental model of sepsis. *Shock* **27**, 397–401.
19. Lyuksutova OI, Murphey ED, Toliver-Kinsky TE, *et al.* (2005) Glucan phosphate treatment attenuates burn-induced inflammation and improves resistance to *Pseudomonas aeruginosa* burn wound infection. *Shock* **23**, 224–232.
20. Soltys J & Quinn MT (1999) Modulation of endotoxin- and enterotoxin-induced cytokine release by *in vivo* treatment with beta-(1,6)-branched beta-(1,3)-glucan. *Infect Immun* **67**, 244–252.
21. Toklu HZ, Sehirli AO, Velioglu-Ogunc A, *et al.* (2006) Acetaminophen-induced toxicity is prevented by beta-D-glucan treatment in mice. *Eur J Pharmacol* **543**, 133–140.
22. Shah VB, Williams DL & Keshvara L (2009) beta-Glucan attenuates TLR2- and TLR4-mediated cytokine production by microglia. *Neurosci Lett* **458**, 111–115.
23. Sumiyoshi M, Suzuki T & Kimura Y (2009) Protective effects of water-soluble low-molecular-weight beta-(1,3–1,6)D-glucan purified from *Aureobasidium pullulans* GM-NH-1A1 against UFT toxicity in mice. *J Pharm Pharmacol* **61**, 795–800.
24. Ha T, Hua F, Grant D, *et al.* (2006) Glucan phosphate attenuates cardiac dysfunction and inhibits cardiac MIF expression and apoptosis in septic mice. *Am J Physiol Heart Circ Physiol* **291**, H1910–H1918.
25. Kimura Y, Sumiyoshi M, Suzuki T, *et al.* (2007) Effects of water-soluble low-molecular-weight beta-1,3-D-glucan (branch beta-1,6) isolated from *Aureobasidium pullulans* 1A1 strain black yeast on restraint stress in mice. *J Pharm Pharmacol* **59**, 1137–1144.

26. Kimura Y, Sumiyoshi M, Suzuki T, *et al.* (2007) Inhibitory effects of water-soluble low-molecular-weight beta-(1,3–1,6) D-glucan purified from *Aureobasidium pullulans* GM-NH-1A1 strain on food allergic reactions in mice. *Int Immunopharmacol* **7**, 963–972.
27. Futaki N, Arai I, Hamasaka Y, *et al.* (1993) Selective inhibition of NS-398 on prostanoid production in inflamed tissue in rat carrageenan-air-pouch inflammation. *J Pharm Pharmacol* **45**, 753–755.
28. Mima S, Tsutsumi S, Ushijima H, *et al.* (2005) Induction of claudin-4 by nonsteroidal anti-inflammatory drugs and its contribution to their chemopreventive effect. *Cancer Res* **65**, 1868–1876.
29. Krawisz JE, Sharon P & Stenson WF (1984) Quantitative assay for acute intestinal inflammation based on myeloperoxidase activity. Assessment of inflammation in rat and hamster models. *Gastroenterology* **87**, 1344–1350.
30. Tanaka K, Namba T, Arai Y, *et al.* (2007) Genetic evidence for a protective role for heat shock factor 1 and heat shock protein 70 against colitis. *J Biol Chem* **282**, 23240–23252.
31. Bradford MM (1976) A rapid and sensitive method for the quantitation of microgram quantities of protein utilizing the principle of protein–dye binding. *Anal Biochem* **72**, 248–254.
32. Salimuddin, Nagasaki A, Gotoh T, *et al.* (1999) Regulation of the genes for arginase isoforms and related enzymes in mouse macrophages by lipopolysaccharide. *Am J Physiol* **277**, E110–E117.
33. Nagasaki A, Gotoh T, Takeya M, *et al.* (1996) Coinduction of nitric oxide synthase, argininosuccinate synthetase, and argininosuccinate lyase in lipopolysaccharide-treated rats. RNA blot, immunoblot, and immunohistochemical analyses. *J Biol Chem* **271**, 2658–2662.
34. Tsutsumi S, Tomisato W, Takano T, *et al.* (2002) Gastric irritant-induced apoptosis in guinea pig gastric mucosal cells in primary culture. *Biochim Biophys Acta* **1589**, 168–180.
35. Corfield AP, Myerscough N, Longman R, *et al.* (2000) Mucins and mucosal protection in the gastrointestinal tract: new prospects for mucins in the pathology of gastrointestinal disease. *Gut* **47**, 589–594.
36. Byrd JC & Bresalier RS (2004) Mucins and mucin binding proteins in colorectal cancer. *Cancer Metastasis Rev* **23**, 77–99.
37. Kim HP, Wang X, Zhang J, *et al.* (2005) Heat shock protein-70 mediates the cytoprotective effect of carbon monoxide: involvement of p38 beta MAPK and heat shock factor-1. *J Immunol* **175**, 2622–2629.
38. Wang X, Khaleque MA, Zhao MJ, *et al.* (2006) Phosphorylation of HSF1 by MAPK-activated protein kinase 2 on serine 121, inhibits transcriptional activity and promotes HSP90 binding. *J Biol Chem* **281**, 782–791.
39. Rice PJ, Adams EL, Ozment-Skelton T, *et al.* (2005) Oral delivery and gastrointestinal absorption of soluble glucans stimulate increased resistance to infectious challenge. *J Pharmacol Exp Ther* **314**, 1079–1086.
40. Chen H, Wu Y, Zhang Y, *et al.* (2006) Hsp70 inhibits lipopolysaccharide-induced NF-kappaB activation by interacting with TRAF6 and inhibiting its ubiquitination. *FEBS Lett* **580**, 3145–3152.
41. Weiss YG, Bromberg Z, Raj N, *et al.* (2007) Enhanced heat shock protein 70 expression alters proteasomal degradation of IkappaB kinase in experimental acute respiratory distress syndrome. *Crit Care Med* **35**, 2128–2138.
42. Asano T, Tanaka K, Yamakawa N, *et al.* (2009) HSP70 confers protection against indomethacin-induced lesions of the small intestine. *J Pharmacol Exp Ther* **330**, 458–467.
43. Matsuda M, Hoshino T, Yamashita Y, *et al.* (2010) Prevention of UVB radiation-induced epidermal damage by expression of heat shock protein 70. *J Biol Chem* **285**, 5848–5858.
44. Jana NR, Tanaka M, Wang G, *et al.* (2000) Polyglutamine length-dependent interaction of Hsp40 and Hsp70 family chaperones with truncated N-terminal huntingtin: their role in suppression of aggregation and cellular toxicity. *Hum Mol Genet* **9**, 2009–2018.
45. Morimoto RI & Santoro MG (1998) Stress-inducible responses and heat shock proteins: new pharmacologic targets for cytoprotection. *Nat Biotechnol* **16**, 833–838.
46. Adachi H, Katsuno M, Minamiyama M, *et al.* (2003) Heat shock protein 70 chaperone overexpression ameliorates phenotypes of the spinal and bulbar muscular atrophy transgenic mouse model by reducing nuclear-localized mutant androgen receptor protein. *J Neurosci* **23**, 2203–2211.
47. Ohkawara T, Nishihira J, Takeda H, *et al.* (2005) Geranylgeranylacetone protects mice from dextran sulfate sodium-induced colitis. *Scand J Gastroenterol* **40**, 1049–1057.
48. Katsuno M, Sang C, Adachi H, *et al.* (2005) Pharmacological induction of heat-shock proteins alleviates polyglutamine-mediated motor neuron disease. *Proc Natl Acad Sci U S A* **102**, 16801–16806.

British Journal of Nutrition

Neurobiology of Disease

Suppression of Alzheimer's Disease-Related Phenotypes by Expression of Heat Shock Protein 70 in Mice

Tatsuya Hoshino,[1] Naoya Murao,[1] Takushi Namba,[1] Masaya Takehara,[1] Hiroaki Adachi,[2] Masahisa Katsuno,[2] Gen Sobue,[2] Takahide Matsushima,[3] Toshiharu Suzuki,[3] and Tohru Mizushima[1]

[1]Graduate School of Medical and Pharmaceutical Sciences, Kumamoto University, Kumamoto 862-0973, Japan, [2]Nagoya University Graduate School of Medicine, Nagoya 466-8550, Japan, and [3]Graduate School of Pharmaceutical Sciences, Hokkaido University, Sapporo 060-0812, Japan

Amyloid-β peptide (Aβ) plays an important role in the pathogenesis of Alzheimer's disease (AD). Aβ is generated by proteolysis of β-amyloid precursor protein (APP) and is cleared by enzyme-mediated degradation and phagocytosis by microglia and astrocytes. Some cytokines, such as TGF-β1, stimulate this phagocytosis. In contrast, cellular upregulation of HSP70 expression provides cytoprotection against Aβ. HSP70 activity in relation to inhibition of Aβ oligomerization and stimulation of Aβ phagocytosis has also been reported. Although these *in vitro* results suggest that stimulating the expression of HSP70 could prove effective in the treatment of AD, there is a lack of *in vivo* evidence supporting this notion. In this study, we address this issue, using transgenic mice expressing HSP70 and/or a mutant form of APP (APPsw). Transgenic mice expressing APPsw showed less of an apparent cognitive deficit when they were crossed with transgenic mice expressing HSP70. Transgenic mice expressing HSP70 also displayed lower levels of Aβ, Aβ plaque deposition, and neuronal and synaptic loss than control mice. Immunoblotting experiments and direct measurement of β- and γ-secretase activity suggested that overexpression of HSP70 does not affect the production Aβ. In contrast, HSP70 overexpression did lead to upregulation of the expression of Aβ-degrading enzyme and TGF-β1 both *in vivo* and *in vitro*. These results suggest that overexpression of HSP70 in mice suppresses not only the pathological but also the functional phenotypes of AD. This study provides the first *in vivo* evidence confirming the potential therapeutic benefit of HSP70 for the prevention or treatment of AD.

Introduction

Alzheimer's disease (AD) is characterized pathologically by the accumulation of neurofibrillary tangles and senile plaques, the latter of which are composed of amyloid-β peptide (Aβ), such as Aβ40 and Aβ42 (Hardy and Selkoe, 2002; Mattson, 2004). To generate Aβ, β-amyloid precursor protein (APP) is first cleaved by β-secretase and then by γ-secretase (Hardy and Selkoe, 2002; Mattson, 2004). Aβ can be cleared from the brain via three main pathways: degradation by enzymes, such as neprilysin, insulin-degrading enzyme (IDE), and endothelin-converting enzyme 2 (ECE-2), phagocytosis by microglia and astrocytes, and transport into the blood and lymph nodes (Miners et al., 2008; Zlokovic, 2008; Rodríguez et al., 2009). However, monomeric Aβ easily self-assembles to form oligomers, protofibrils, and fibrils, and it is now believed that less aggregated forms of Aβ, such as oligomers and protofibrils, are more important than the highly aggregated forms (Haass and Selkoe, 2007). Therefore, cellular factors that affect the production and clearance of Aβ and/or oligomerization of Aβ may be good targets for the development of drugs to prevent or treat AD.

When cells are exposed to stressors, heat shock proteins (HSPs) are induced, and the cellular upregulation of their expression, especially that of HSP70, provides resistance as the HSPs refold or degrade denatured proteins produced by the stressors (Morimoto and Santoro, 1998; Muchowski and Wacker, 2005). Not only AD but also other neurodegenerative diseases display aggregation of proteins, and overexpression of HSP70 (polyglutamine diseases) or HSP104 (Parkinson's disease) in animal models suppresses the aggregation of each pathogenic protein and ameliorates the corresponding disease symptoms (Adachi et al., 2003; Katsuno et al., 2005; Muchowski and Wacker, 2005; Lo Bianco et al., 2008). An increased level of expression of HSPs, such as small HSPs and HSP70 in the brain of AD patients, has been reported in a number of studies (Perez et al., 1991; Muchowski and Wacker, 2005), with *in vitro* experiments suggesting that expression of HSPs, in particular HSP70, could suppress the progression of AD (Magrané et al., 2004; Muchowski and Wacker, 2005; Evans et al., 2006; Kumar et al., 2007; Yoshiike et al., 2008). In terms of *in vivo* studies, the effect of overexpression of HSPs on the pathogenesis of AD has not been examined in vertebrate models. In this study, we investigated the effect of overexpression of HSP70 on AD-related phenotypes, using transgenic mice expressing HSP70 and/or a mutant (Swedish) type of APP (APPsw). Our results demonstrate that overexpression of HSP70 suppresses not only the pathological phenotypes of AD

Received Oct. 19, 2010; revised Jan. 11, 2011; accepted Jan. 14, 2011.

This work was supported by Grants-in-Aid for Scientific Research from the Ministry of Health, Labour, and Welfare of Japan, as well as the Japan Science and Technology Agency, Grants-in-Aid for Scientific Research from the Ministry of Education, Culture, Sports, Science and Technology, Japan. We thank Drs. M. Staufenbiel (Novartis Institutes for BioMedical Research, Basel, Switzerland), and C. E. Angelidis and G. N. Pagoulatos (University of Ioannina, Ioannina, Greece) for providing transgenic mice.

Correspondence should be addressed to Tohru Mizushima, Graduate School of Medical and Pharmaceutical Sciences, Kumamoto University, 5-1 Oe-honmachi, Kumamoto 862-0973, Japan. E-mail: mizu@gpo.kumamoto-u.ac.jp.

DOI:10.1523/JNEUROSCI.5478-10.2011

but also the resultant cognitive deficits, possibly through its effects on antiaggregation, neuroprotection, and stimulation of Aβ clearance.

Materials and Methods

Materials. Eagle's minimal essential medium (EMEM) was obtained from Nissui Pharmaceutical. A fluorescent substrate for β-secretase [H_2N-Arg-Glu-(EDANS)-Glu-Val-Asn-Leu-Asp-Ala-Glu-Phe-Lys-(DABCYL)-Arg-O] was purchased from Calbiochem and that for γ-secretase [Nma-Gly-Gly-Val-Val-Ile-Ala-Thr-Val-Lys(Dnp)-D-Arg-D-Arg-D-Arg-NH_2] and synthetic Aβ were obtained from Peptide Institute. Alexa Fluor 488 goat anti-mouse IgG, Neurobasal medium, B27, and an antibody to Aβ oligomer (A11) were purchased from Invitrogen. Sandwich ELISA (sELISA) kit for Aβ oligomers was obtained from Immunobiological Laboratories. An antibody to actin was obtained from Santa Cruz. Fetal bovine serum (FBS), thioflavin-S, and antibodies to the C-terminal fragment (CTF) of APP and synaptophysin were purchased from Sigma-Aldrich. An antibody to Aβ (6E10) came from Covance Research Products. An antibody to HSP70 was from Assay Designs, and those against neuronal nuclei (NeuN) and presenilin 1 (PS1) were from Millipore Bioscience Research Reagents. The RNeasy kit was obtained from QIAGEN. PrimeScript first-strand cDNA Synthesis kit was from Takara Bio, and iQ SYBR Green Supermix was purchased from Bio-Rad. ELISA kits for tumor necrosis factor-α (TNF-α), interleukin-1β (IL-1β), and IL-6 were from Pierce. An ELISA kit for TGF-β1 was obtained from R&D Systems. Sandwich ELISA kits for Aβ40 and Aβ42 and ara-C (cytarabine) were from Wako. Mounting medium for immunohistochemical analysis (VECTASHIELD) was from Vector Laboratories. Mayer's hematoxylin and mounting medium for histological examination (malinol) were purchased from Muto Pure Chemicals. The Envision kit was from Dako.

Animals. Transgenic mice that express APPsw (APP23, C57BL/6) were a gift from Dr. M. Staufenbiel (Novartis Institutes for BioMedical Research, Basel, Switzerland) (Sturchler-Pierrat et al., 1997). Transgenic mice expressing HSP70 were gifts from Drs. C. E. Angelidis and G. N. Pagoulatos (University of Ioannina, Ioannina, Greece) and crossed with C57BL/6 wild-type mice (WT/WT) 10 times to generate WT/HSP70 mice (Tanaka et al., 2007). APP23 male mice were crossed with WT/HSP70 female mice to generate APPsw/HSP70 mice. Parallel crosses were made between APP23 mice and WT/WT mice to generate APPsw/WT animals. All experiments in this study were done using female mice.

The experiments and procedures described here were performed in accordance with the *Guide for the Care and Use of Laboratory Animals* as adopted and promulgated by the National Institutes of Health and were approved by the Animal Care Committee of Kumamoto University.

Morris water maze test. The Morris water maze test was conducted in a circular 90-cm-diameter pool filled with water at a temperature of 22.0 ± 1°C, as described previously (Kobayashi et al., 2000; Huang et al., 2006), with minor modifications. In the hidden platform test, a circular platform (10 cm in diameter) was submerged 0.5 cm below water level. Swimming paths were tracked for 60 s with a camera and stored in a computer (Video Tracking System CompACT VAS/DV; Muromachi kikai). The mice were given four trials (one block) per day for 7 consecutive days, during which the platform was left in the same position. The time taken to reach the platform (escape latency) was measured, and the average of four trials was determined.

Twenty-four hours after the last trial of the hidden platform test, the mice were subjected to a transfer test in which the platform was removed, and their swimming path was recorded for 60 s. Percentage search time for each quadrant and crossing time in the area where the platform had been located were determined.

sELISA for Aβ or Aβ oligomer and ELISA for cytokines. Cells were cultured for 48 h, and the conditioned medium was subjected to sELISA for Aβ, as described previously (Tomita et al., 1998b; Hoshino et al., 2007a).

Aβ40, Aβ42, and cytokine levels in the brain were determined as described previously (Iwata et al., 2004). Briefly, the brain hemispheres were homogenized in 50 mM Tris/HCl buffer, pH 7.6, containing 150 mM NaCl, and then centrifuged. Guanidine/HCl (0.5 M, final concentration) was added to the supernatants (soluble fractions). The precipitates were solubilized by sonication in 6 M guanidine/HCl, after which the solubilized pellet was centrifuged and the resulting supernatant diluted (insoluble fractions). The amount of Aβ40 and Aβ42 in each fraction was determined by sELISA. An ELISA assay for Aβ oligomers or cytokines was performed on the soluble fractions (but without guanidine/HCl), according to the manufacturer's instructions.

Thioflavin-S staining and immunohistochemical analyses. The brain hemispheres were fixed in 4% buffered paraformaldehyde and embedded in paraffin before being cut into 4-μm-thick sections, which were then deparaffinized and washed in PBS.

For thioflavin-S staining, sections were stained with 1% thioflavin-S solution. Samples were mounted with malinol and inspected using a BX51 microscope (Olympus). Fluorescence microscopic images at region (1.0 mm^2) in the hippocampus and cerebral cortex were used to calculate the area stained with thioflavin-S using the LuminaVision (Mitani). By determining the threshold optical density, we divided into thioflavin-S-positive and -negative area and the percentage of thioflavin-S-positive area to total area was determined. We prepared three sections per mouse and calculated the average of values in three sections.

For immunohistochemical analysis to detect NeuN and HSP70, sections were incubated with 0.3% hydrogen peroxide in methanol for removal of endogenous peroxidase. They were then blocked with 2.5% goat serum for 10 min, and incubated for 12 h with antibody to NeuN (1:1000 dilution) or HSP70 (1:100 dilution) in the presence of 2.5% bovine serum albumin (BSA), followed by incubation for 1 h with peroxidase-labeled polymer conjugated to goat anti-mouse (for NeuN) or anti-rabbit (for HSP70) Ig. 3,3′-Diaminobenzidine was applied to the sections, which were then incubated with Mayer's hematoxylin. Samples were mounted with malinol and inspected using a BX51 microscope. NeuN-positive cells in the pyramidal cell layer of the hippocampal CA3 region (within 500 μm from the edge of the dentate gyrus) were counted. We prepared three sections per mouse and calculated the average of values in three sections.

For immunohistochemical analysis to detect synaptophysin, sections were blocked with 2.5% goat serum (v/v) for 10 min, incubated for 12 h with antibody to synaptophysin (1:200 dilution) in the presence of 2.5% BSA, and then incubated with Alexa Fluor 488 goat anti-mouse IgG. Samples were mounted with VECTASHIELD and inspected with the aid of a BX51 fluorescence microscope. Fluorescence intensity in area (100 × 150 μm) of the hippocampal CA3 region was determined using LuminaVision and shown relative to fluorescence intensity in wild-type mice. We prepared three sections per mouse and calculated the average of values in three sections.

Immunoblotting analysis. Whole-cell extracts were prepared as described previously (Hoshino et al., 2003). The protein concentration of each sample was determined by the Bradford method (Bradford, 1976). Samples were applied to SDS polyacrylamide gels (Tris/tricine gel for detection of Aβ, CTFα, and CTFβ or Tris/glycine gel for detection of other proteins) and subjected to electrophoresis, after which proteins were immunoblotted with each antibody.

A dot blotting assay for Aβ oligomer was performed on the soluble fractions (but without guanidine/HCl), as described previously (Wang et al., 2007). Proteins (4 μg) of soluble fractions were applied to nitrocellulose membrane, after which proteins were detected with antibody against Aβ oligomer (A11).

β- and γ-secretase-mediated peptide cleavage assay. β- and γ-secretase activity was monitored as previously reported (Fukumoto et al., 2002; Farmery et al., 2003). Solubilized membranes were incubated for 1 h at 37°C in 200 μl of 50 mM acetate buffer, pH 4.1, containing 100 mM sodium chloride, 0.025% BSA, and 10 μM β-secretase fluorescent substrate or for 4 h at 37°C in 200 μl of 50 mM Tris/HCl buffer, pH 6.8, containing 2 mM EDTA, 0.25% CHAPSO (3-[(3-cholamidopropyl)dimethylammonio]-2-hydroxy-1-propanesulfonate), and 10 μM γ-secretase fluorescent substrate. Fluorescence was measured using a plate reader (Fluostar Galaxy; BMG Labtech) with an excitation wavelength of 355 nm and an emission wavelength of 510 nm (for β-secretase) or 440 nm (for γ-secretase).

Real-time reverse transcription-PCR analysis. Real-time reverse transcription (RT)-PCR was performed as previously described (Mima et al., 2005) with some modifications. Total RNA was extracted from the brain

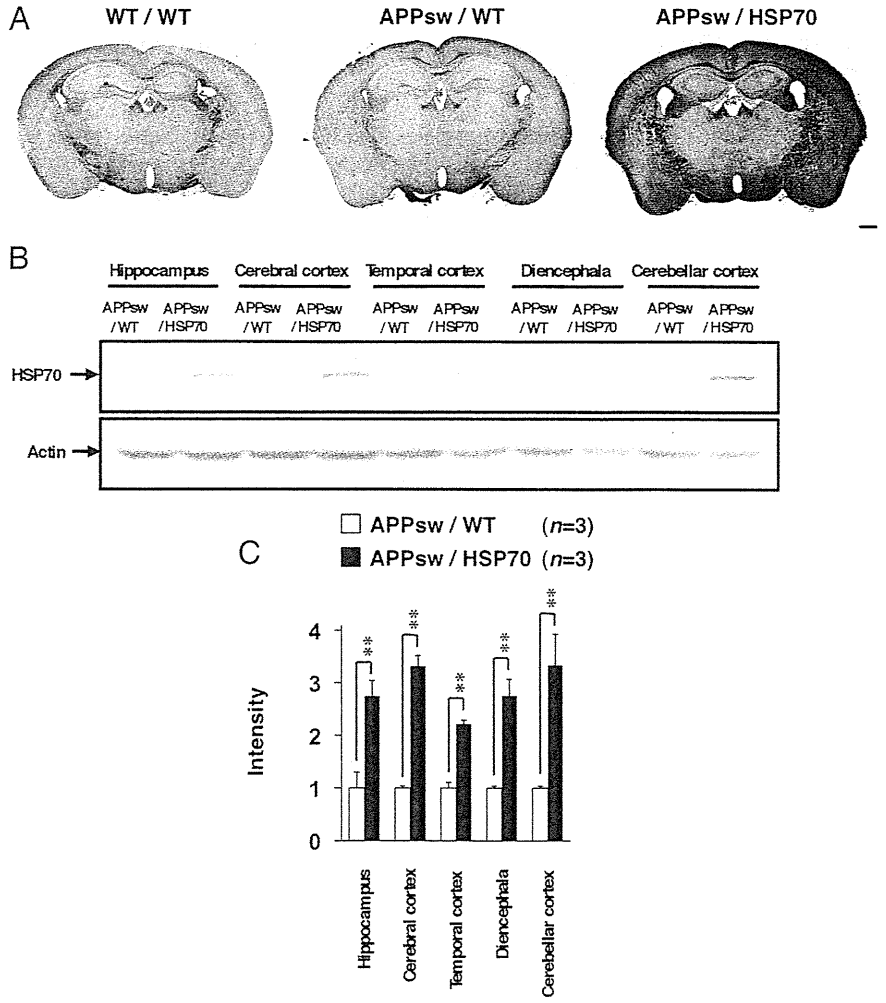

Figure 1. Expression of HSP70 in the brain. ***A***, ***B***, Brains were removed from WT/WT, APPsw/WT, and APPsw/HSP70 mice at the age of 18 months. ***A***, Sections were prepared and subjected to immunohistochemical analysis with an antibody to HSP70. Scale bar, 500 μm. ***B***, Brains were divided into fractions containing the hippocampus, cerebral cortex, temporal cortex, diencephala, and cerebellar cortex. Whole-cell extracts were then prepared from each fraction and subjected to immunoblotting with an antibody to HSP70 or actin. ***C***, The band intensity of HSP70 was determined, corrected with that of actin, and expressed relative to the control ($n = 3$). $^{**}p < 0.01$. Error bars indicate SEM.

or cultured cells using an RNeasy kit according to the manufacturer's protocol. Samples (1 μg of RNA) were reverse-transcribed using a first-strand cDNA synthesis kit. Synthesized cDNA was used in real-time RT-PCR (Chromo 4 instrument; Bio-Rad) experiments using iQ SYBR GREEN Supermix, and then analyzed with Opticon Monitor Software. Specificity was confirmed by electrophoretic analysis of the reaction products and by inclusion of template- or reverse transcriptase-free controls. To normalize the amount of total RNA present in each reaction, glyceraldehyde-3-phosphate dehydrogenase (GAPDH) cDNA was used as an internal standard.

Primers were designed using the Primer3 website. The primers used were as follows (name: forward primer, reverse primer): *gapdh*: 5′-aactttggcattgtggaagg-3′, 5′-acacattgggggtaggaaca-3′; *neprilysin*: 5′-gcagcctcagccgaaactac-3′, 5′-caccgtctccatgttgcagt-3′; *ide*: 5′-accaggaaatgttggctgtc-3′, 5′-tctgagaggggaactctcca-3′; *ece-2*: 5′-gctatgcccatgtacccagt-3′, 5′-tggcatccagagtaccttc-3′; *il-1β*: 5′-gatcccaagcaatacccaaa-3′, 5′-ggggaactctgcagactcaa-3′; *il-6*: 5′-ctggagtcacagaaggagtgg-3′, 5′-ggtttgccgagtagatctcaa-3′; *tnf-α*: 5′-cgtcagccgatttgctatct-3′, 5′-cggactccgcaaagtctaag-3′; *tgf-β1*: 5′-tgacgtcactggagtacgg-3′, 5′-ggttcatgtcatggatggtgc-3′.

Cell culture. The primary culture of cortical neurons was done as described previously (Saito et al., 2008). The cortex of embryonic day 15.5 mice was dissected. Neurons were spread in a buffer containing papain and cultured at 5×10^4 cells cm^{-2} in Neurobasal medium containing B27 and antibiotics on poly-D-lysine-coated dishes.

Primary cultures of microglia and astrocytes were prepared as described previously (Kauppinen and Swanson, 2005). The cortex of 1-d-old mice was dissected. Cells were spread in a buffer containing papain and DNase and cultured at 1×10^6 cells cm^{-2} in EMEM containing 10 mM HEPES/KOH and 10% FBS for 2 weeks. Microglial cells were obtained by mildly shaking and collecting the floating cells. For preparation of astrocytes, cells were further incubated in EMEM containing 10 mM HEPES/KOH, 10% FBS, and 20 μM ara-C for 3 d to induce microglial cell death.

Statistical analysis. All values are expressed as the mean ± SEM or SD. Two-way ANOVA followed by Tukey's test was used to evaluate differences between more than three groups. Student's t test for unpaired results was used for the evaluation of differences between two groups. Differences were considered to be significant for values of $p < 0.05$.

Results

Effect of overexpression of HSP70 on cognitive function in transgenic mice expressing APPsw

To examine the effect of overexpression of HSP70 on the pathogenesis of AD, we used transgenic mice expressing APPsw (APP23, AD model mice) crossed to transgenic mice that express human HSP70 under the control of the human β-actin promoter (Plumier et al., 1995). The overexpression of HSP70 in the mice has been demonstrated in various organs, including the brain (Plumier et al., 1997). We first confirmed the expression of HSP70 in the brain by immunohistochemical analysis. As shown in Figure 1*A*, a higher level of HSP70 expression was observed in various brain regions, including the hippocampus and cerebral cortex, in the HSP70 transgenic mice (APPsw/HSP70) at the age of 18 months when compared with the control animals (WT/WT and APPsw/WT). We also compared the level of HSP70 in various parts of the brain by immunoblotting. Higher levels of HSP70 were observed in all regions of the brain tested (hippocampus, cerebral cortex, temporal cortex, diencephala, and cerebellar cortex) in the APPsw/HSP70 mice at the age of 18 months than in the APPsw/WT mice (Fig. 1*B*). Similar results were observed APPsw/HSP70 mice at the age of 12 months (supplemental Fig. 1, available at www.jneurosci.org as supplemental material).

We then used a Morris water maze to examine the effect of overexpression of HSP70 on spatial learning and memory. Four strains of mice (WT/WT, WT/HSP70, APPsw/WT, and APPsw/HSP70) were trained to learn the location of a hidden platform four times per day for 7 d, and the time required to reach the platform (escape latency) was measured. As shown in Figure 2*A*, APPsw/WT mice took a significantly longer time than WT/WT mice to reach the platform, a result that is consistent with previous reports (Van Dam et al., 2003) and suggests a deficiency in spatial learning and memory in the former group. This impaired ability of APPsw/WT mice to reach the hidden platform did not reflect reduced swimming ability, as swimming speed and ability to locate a visible platform were indistinguishable between the

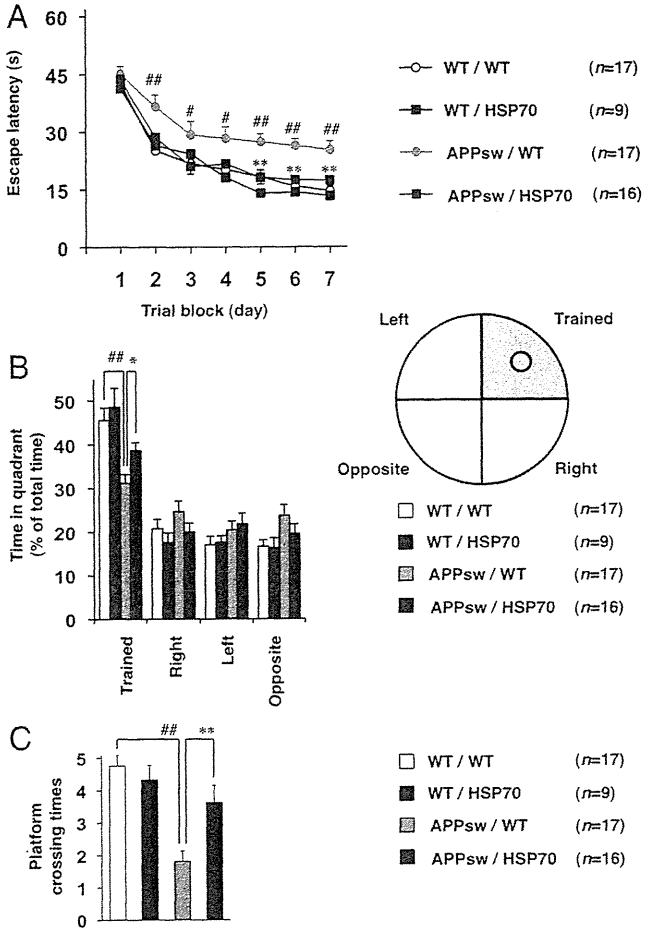

Figure 2. Effects of overexpression of HSP70 on spatial learning and memory in transgenic mice expressing APPsw. Cognitive behavioral tests were performed, using the Morris water maze, on 12-month-old WT/WT (n = 17), WT/HSP70 (n = 9), APPsw/WT (n = 17), and APPsw/HSP70 mice (n = 16) as described in Materials and Methods. The average (4 tests) escape latency in each trial block was measured for 7 d (***A***), after which the mice were subjected to a transfer test in which the platform was removed. ***B***, ***C***, The spatial memory for a platform location was estimated by percentage search time for each quadrant (the platform had been located in the "trained" quadrant) (***B***) or platform crossing times (***C***). Values are given as mean ± SEM. $^{**}p < 0.01$, $^{*}p < 0.05$, versus APPsw/WT mice; $^{\#\#}p < 0.01$, $^{\#}p < 0.05$, versus WT/WT mice.

four strains of mice (data not shown). APPsw/HSP70 mice took a significantly shorter time to reach the platform than APPsw/WT mice (Fig. 2*A*). Furthermore, there was no significant difference in the escape latency between APPsw/HSP70 and WT/WT mice or between WT/HSP70 and WT/WT mice (Fig. 2*A*). These results suggest that expression of APPsw leads to disturbances in spatial learning and memory, an effect that can be ameliorated by overexpression of HSP70.

We next performed a transfer test to estimate the spatial memory of platform location. After a 7 d training period (see above), each mouse was subjected to a Morris water maze test in which the platform was removed and the percentage search time for each quadrant was measured. As shown in Figure 2*B*, the ratio of time spent in the trained quadrant was lower for the APPsw/WT group than for either the WT/WT or the APPsw/HSP70 mice. Furthermore, the crossing time of the area where the platform had been located, another indicator of spatial memory, was lower in the APPsw/WT group than in the WT/WT and APPsw/HSP70 cohorts (Fig. 2*C*). Again, there was no significant difference in these indices between WT/HSP70 and WT/WT mice (Fig. 2*B*,*C*). These results confirm the notion that overexpression of HSP70 ameliorates the spatial memory deficits of transgenic mice expressing APPsw.

Effect of overexpression of HSP70 on Aβ accumulation and neuronal and synaptic loss in transgenic mice expressing APPsw

The amounts of Aβ40 and Aβ42 in soluble and insoluble brain fractions were compared between APPsw/HSP70 and APPsw/WT mice by sELISA. As shown in Figure 3*A*, the levels of Aβ40 and Aβ42 in both brain fractions were lower in the APPsw/HSP70 group than in the APPsw/WT mice.

We then examined the effect of overexpression of HSP70 on plaque deposition and neurotoxicity in APP23 mice. Because plaque deposition and neurotoxicity (neuronal and synaptic loss) were not observed in APP23 mice at the age of 12 months (data not shown), we used mice at the age of 18 months. At first, we compared the level of Aβ plaque deposition in the brain between APPsw/HSP70 mice and APPsw/WT mice by thioflavin-S staining. As shown in Figure 3, *B* and *C*, the level of Aβ plaque deposition in both the hippocampus and the cerebral cortex was much lower in the APPsw/HSP70 mice than in the APPsw/WT animals. Very little Aβ plaque deposition was observed in WT/WT mice (Fig. 3*B*,*C*).

We then compared the number of neurons in the hippocampal CA3 region of APPsw/HSP70 and APPsw/WT mice by NeuN staining. As shown in Figure 3, *D* and *E*, the number of NeuN-positive cells (neurons) was significantly higher in the WT/WT and APPsw/HSP70 brain sections than in the APPsw/WT tissue, suggesting that Aβ-induced neuronal loss was ameliorated by overexpression of HSP70. We also estimated the number of synapses based on synaptophysin staining. The level of synaptophysin staining was higher in sections from both WT/WT and APPsw/HSP70 mice than from APPsw/WT mice (Fig. 3*F*,*G*), indicating that overexpression of HSP70 suppresses Aβ-induced synaptic loss. Together, the results in Figure 3 suggest that overexpression of HSP70 decreases the level of Aβ and Aβ plaque deposition in the brain and protects it against Aβ-induced neurotoxicity.

Effect of overexpression of HSP70 on the production and oligomerization of Aβ

To understand the molecular mechanism governing the HSP70-mediated decrease in levels of Aβ and Aβ plaque deposition, we examined the effect of overexpression of HSP70 on the production of Aβ. In general, production of Aβ is regulated by either modification of APP or modulation of secretase activity. We first examined the effect of overexpression of HSP70 on the maturation of APP, an essential step in the production of Aβ. The mature (*N*- and *O*-glycosylated) and immature (*N*-glycosylated alone) forms of APP (mAPP and imAPP, respectively) can be separated by SDS-PAGE on the basis of molecular weight (Tomita et al., 1998a). As shown in Figure 4*A*, mAPP and imAPP were detected in transgenic mice expressing APPsw, and the total amount of APP and the ratio of mAPP and imAPP were indistinguishable between APPsw/HSP70 mice and APPsw/WT animals. We also found that overexpression of HSP70 did not affect the level of PS1 (Fig. 4*A*).

Next, we tested the notion that overexpression of HSP70 affects production of Aβ through modulation of secretase activity by comparing the amount of CTFs, the secreted forms of APP that are generated by α or β-secretase (CTFα or CTFβ, respectively, known as an indirect index of the secretase activity), between APPsw/HSP70 and APPsw/WT mice. Under our experimental conditions, we could not detect the band of CTFγ. As shown in Figure 4*B*, CTFα and CTFβ were detected in transgenic mice ex-

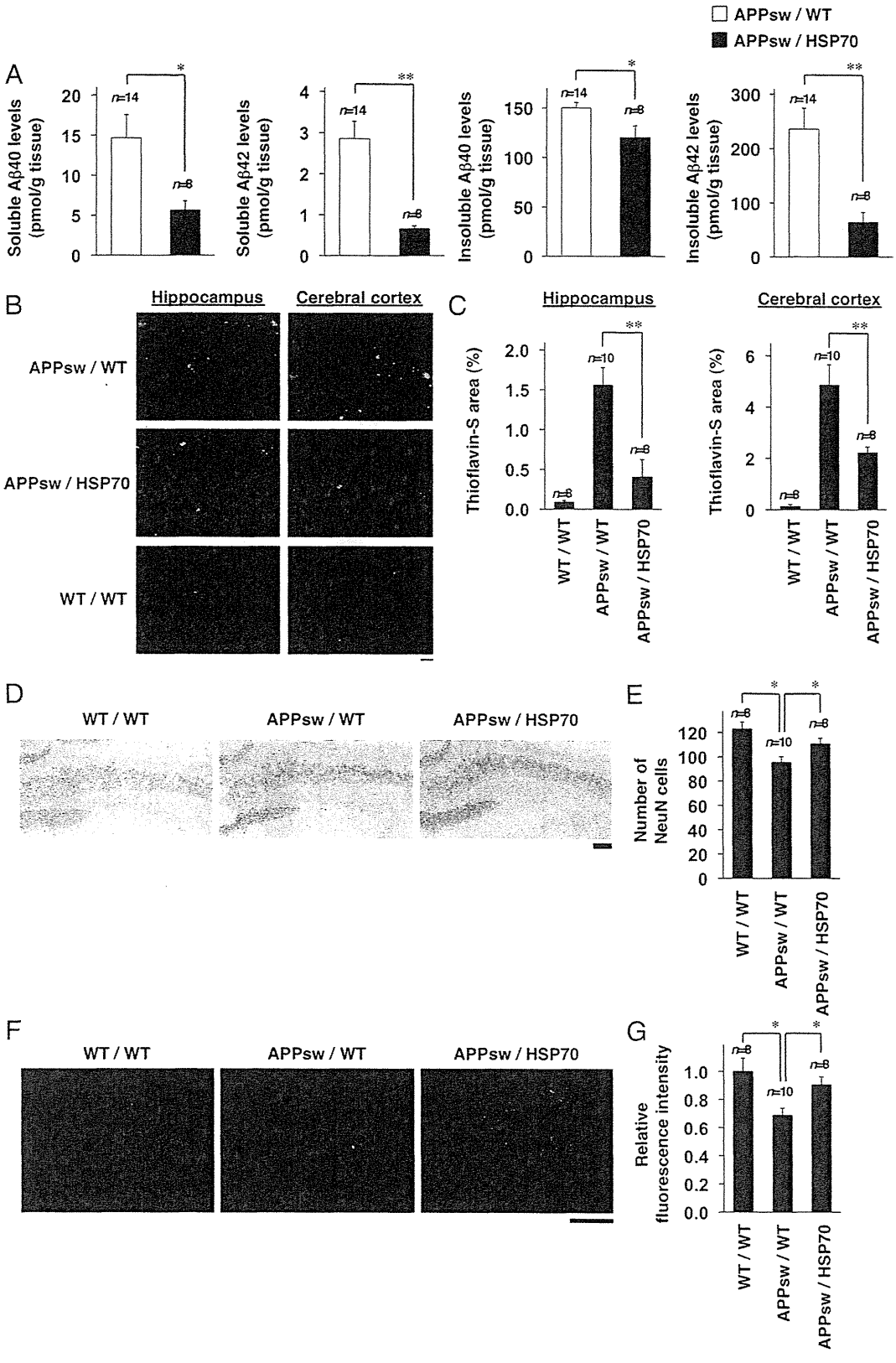

Figure 3. Effects of HSP70 overexpression on Aβ levels, Aβ plaque deposition, and neuronal and synaptic loss in the brain of transgenic mice expressing APPsw. ***A***, Soluble and insoluble fractions were prepared from the brains of 12-month-old APPsw/WT ($n = 14$) and APPsw/HSP70 mice ($n = 8$). The amounts of Aβ40 and Aβ42 in each fraction were determined by sELISA as described in Materials and Methods. ***B***, ***D***, ***F***, Brain sections were prepared from 18-month-old APPsw/WT ($n = 10$), APPsw/HSP70 ($n = 8$), and WT/WT mice ($n = 8$), and then subjected to thioflavin-S staining (***B***) and immunohistochemical analysis with an antibody to NeuN (***D***) or synaptophysin (***F***). Scale bars: ***B***, 200 μm; ***D***, 100 μm; ***F***, 50 μm. ***C***, ***E***, ***G***, Relative area stained with thioflavin-S (***C***), number of NeuN-positive cells in hippocampal CA3 region (***E***), and relative fluorescence intensity (synaptophysin) in hippocampal CA3 region (***G***) (3 sections per brain) were determined. Values are given as mean ± SEM. $^{**}p < 0.01$; $^{*}p < 0.05$.

pressing APPsw, and the amounts of CTFα and CTFβ were indistinguishable between the APPsw/HSP70 and APPsw/WT mice. We then directly measured β- and γ-secretase activity, using the APP-derived fluorescent substrate of each secretase (Hoshino et al., 2009). As shown in Figure 4*C*, the activity was indistinguishable between the APPsw/HSP70 and APPsw/WT groups. These results suggest that overexpression of HSP70 does not affect the production of Aβ.

To test this idea *in vitro*, we prepared primary cultures of neurons from APPsw/HSP70 and APPsw/WT mice and compared the level and modification of APP in the cells, as well as the level of Aβ40 and Aβ42 in the culture medium. We also confirmed the overexpression of HSP70 in primary neurons prepared from APPsw/HSP70 mice (Fig. 4*D*). As shown in Figure 4, *D* and *E*, no significant differences were observed in the total amount of APP, the ratio of mAPP and imAPP, and the levels of Aβ40 and Aβ42 in the primary neuronal cultures between the APPsw/HSP70 and APPsw/WT groups, supporting the idea that overexpression of HSP70 does not affect the production of Aβ.

We then compared the level of Aβ oligomer in the brain of APPsw/HSP70 and APPsw/WT mice by immunoblotting analysis. As shown in Figure 5, *A* and *B*, not only the level of Aβ monomer but also that of Aβ oligomers (dimer, trimer, and hexamer) was lower in the APPsw/HSP70 animals. The decrease in the level of Aβ oligomer in the brain of APPsw/HSP70 was confirmed by ELISA assay for Aβ oligomer (Fig. 5*C*) and dot-blotting assay with antibody that specifically recognizes oligomer form of Aβ (A11) (Fig. 5*D*,*E*). The specificity of this antibody (A11) to Aβ oligomer was suggested by the observation that this antibody did not give positive signals against samples from wild-type mice (without expression of APPsw) (supplemental Fig. 2, available at www.jneurosci.org as supplemental material).

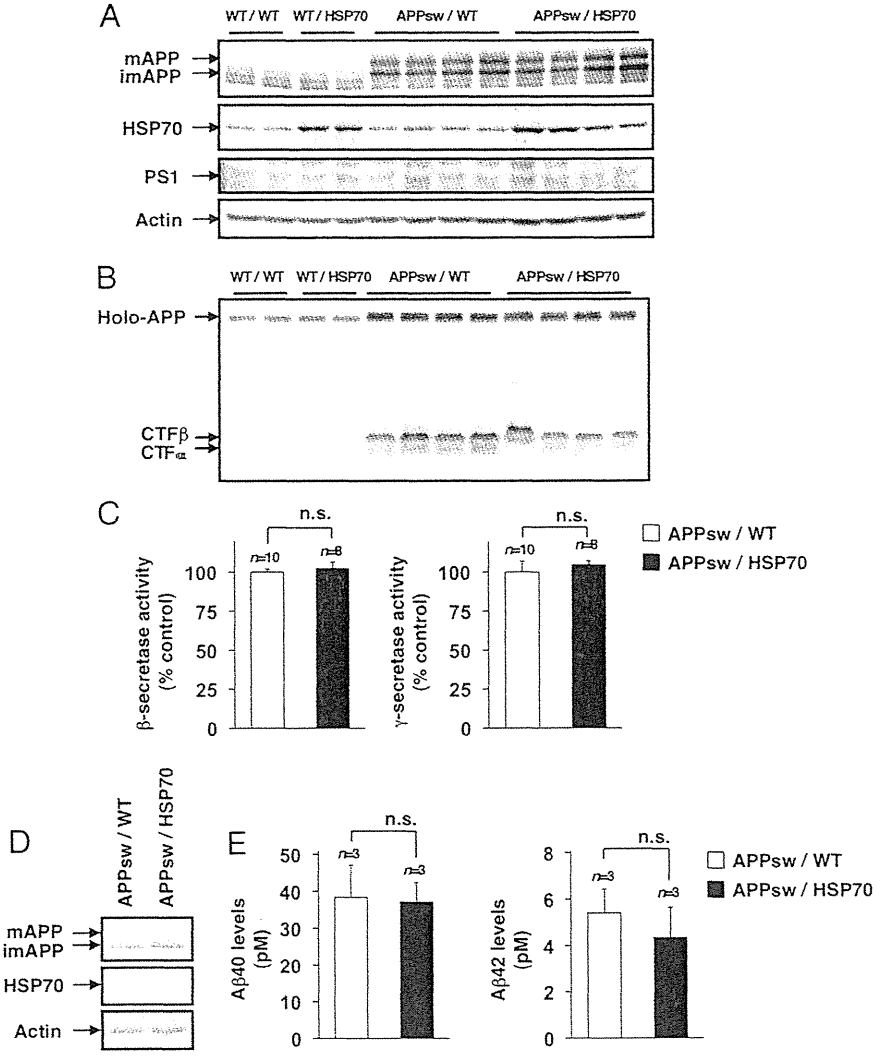

Figure 4. Effects of HSP70 overexpression on the production of Aβ. ***A–C***, Whole-cell extracts (***A***, ***B***) and membrane fractions (***C***) were prepared from the brains of 12-month-old WT/WT, WT/HSP70, APPsw/WT, and APPsw/HSP70 mice. Whole-cell extracts were subjected to immunoblotting with an antibody to APP (***A***, ***B***), HSP70 (***A***), PS1 (***A***), or actin (***A***). Membrane fractions were subjected to a β- or γ-secretase-mediated peptide cleavage assay as described in Materials and Methods [APPsw/WT ($n = 10$) and APPsw/HSP70 mice ($n = 8$)]. Values are given as mean ± SEM. n.s., Not significant (***C***). ***D***, ***E***, Primary neurons prepared from APPsw/WT mice ($n = 3$) and APPsw/HSP70 mice ($n = 3$) were incubated for 7 d. Whole-cell extracts were prepared and subjected to immunoblotting with an antibody to APP, HSP70, or actin (***D***). After incubation for 48 h, the amounts of Aβ40 and Aβ42 in the conditioned medium were determined by sELISA. Values are given as mean ± SD. n.s., Not significant (***E***).

We then examined the colocalization of Hsp70 with APP, Aβ, Aβ oligomer, and Aβ plaque. Intracellular colocalization of HSP70 with APP and Aβ was observed (supplemental Fig. 3*A*,*C*, available at www.jneurosci.org as supplemental material). However, extracellular colocalization of HSP70 with Aβ plaque was not observed so clearly (supplemental Fig. 3*B*,*D*, available at www.jneurosci.org as supplemental material). The intracellular colocalization of HSP70 with Aβ oligomer was also observed in both hippocampus and cerebral cortex (supplemental Fig. 3*E*,*F*, available at www.jneurosci.org as supplemental material).

Effect of overexpression of HSP70 on the expression of genes involving Aβ clearance

As described in Introduction, degradation by enzymes and phagocytosis by microglia and astrocytes are involved in the clearance of Aβ (Miners et al., 2008). We therefore next compared the expression of genes involved in this process. Real-time RT-PCR analysis of brain samples revealed that the mRNA expression of *ide*, but not that of *neprilysin* or *ece-2*, was higher in the APPsw/HSP70 mice than in the APPsw/WT animals (Fig. 6*A*). The upregulation of mRNA expression of *ide* by overexpression of HSP70 was also observed in wild-type mice (without expression of APPsw) (supplemental Fig. 4, available at www.jneurosci.org as supplemental material). We also examined the effect of overexpression of HSP70 on the mRNA expression of *ide* in primary cultures of neurons, astrocytes, and microglia. As shown in Figure 6*B*, the mRNA expression of *ide* was higher in primary astrocyte and microglial cultures prepared from APPsw/HSP70 mice than in those from APPsw/WT mice. In contrast, no significant difference was seen in the neuronal cultures (Fig. 6*B*). These results suggest that the upregulation of *ide* expression is involved in the decrease in the level of Aβ observed in the brain of APPsw/HSP70 mice.